

Nearest neighbor Dirichlet process

Shounak Chattopadhyay^{*1}, Antik Chakraborty^{†1}, and David B. Dunson^{‡1}

¹Department of Statistical Sciences, Duke University

Abstract

There is a rich literature on Bayesian nonparametric methods for unknown densities. The most popular approach relies on Dirichlet process mixture models. These models characterize the unknown density as a kernel convolution with an unknown almost surely discrete mixing measure, which is given a Dirichlet process prior. Such models are very flexible and have good performance in many settings, but posterior computation typically relies on Markov chain Monte Carlo algorithms that can be complex and inefficient. As a simple alternative, we propose a class of nearest neighbor-Dirichlet processes. The approach starts by grouping the data into neighborhoods based on standard algorithms. Within each neighborhood, the density is characterized via a Bayesian parametric model, such as a Gaussian with unknown parameters. Assigning a Dirichlet prior to the weights on these local kernels, we obtain a simple pseudo-posterior for the weights and kernel parameters. A simple and embarrassingly parallel Monte Carlo algorithm is proposed to sample from the resulting pseudo-posterior for the unknown density. Desirable asymptotic properties are shown, and the methods are evaluated in simulation studies and applied to a motivating data set in the context of classification.

KEYWORDS: *Bayesian nonparametric, Density estimation, Dirichlet process mixture, Distributed computing, Embarrassingly parallel, Quasi-posterior, Scalable*

1 Introduction

Bayesian nonparametric methods provide a useful alternative to black box machine learning algorithms, having potential advantages in terms of characterizing uncertainty in inferences

^{*}shounak.chattopadhyay@duke.edu

[†]antik.chakraborty@duke.edu

[‡]dunson@duke.edu

and predictions. However, computation can be slow and unwieldy to implement. Hence, it is important to develop simpler and faster Bayesian nonparametric approaches, and *hybrid* methods that borrow the best of both worlds. For example, if one could use the Bayesian machinery for uncertainty quantification and reduction of mean square errors through shrinkage, while incorporating algorithmic aspects of machine learning approaches, one may be able to engineer a highly effective hybrid. The focus of this article is on proposing such an approach for density estimation, motivated by the successes and limitations of nearest neighbor algorithms and Dirichlet process mixture models.

Nearest neighbor algorithms are popular due to a combination of simplicity and performance. Given a set of n observations $\mathcal{X}^{(n)} = (X_1, \dots, X_n)$ in \mathbb{R}^p , the density at x is estimated as $\hat{f}_{knn}(x) = k/(nV_p R_k^p)$, where k is the number of neighbors of x in $\mathcal{X}^{(n)}$, $R_k = R_k(x)$ is the distance of x from its k th nearest neighbor in $\mathcal{X}^{(n)}$ and V_p is the volume of the p -dimensional unit ball (Loftsgaarden and Quesenberry, 1965; Mack and Rosenblatt, 1979). Refer to Biau and Devroye (2015) for an overview of related estimators and corresponding theory.

Alternatively, following a Bayesian nonparametric approach, one can choose a prior $f \sim \Pi$, with Π chosen to have large support over a set of densities \mathcal{F} . It is important for Π to be interpretable and computationally tractable, and Dirichlet process mixture models provide a convenient choice (Ferguson, 1973; Lo, 1984; Escobar and West, 1995):

$$f(x) = \int \mathcal{K}(x; \theta) dP(\theta), \quad P \sim \text{DP}(\alpha P_0), \quad (1)$$

where $\mathcal{K}(x; \theta)$ is a parametric density with parameters θ , and the mixing measure P is assigned a Dirichlet process prior with precision α and base probability measure P_0 . Under the stick-breaking representation (Sethuraman, 1994), (1) can be equivalently represented as

$$f(x) = \sum_{h=1}^{\infty} \pi_h \mathcal{K}(x; \theta_h), \quad \theta_h \sim P_0, \quad (\pi_h)_{h=1}^{\infty} \sim \text{Stick}(\alpha), \quad (2)$$

which corresponds to a discrete mixture. There are a rich variety of Markov chain Monte Carlo algorithms for posterior computation under (2) (Neal, 2000; Papaspiliopoulos and Roberts, 2008; Jain and Neal, 2004; Ishwaran and James, 2001), and a rich literature on frequentist asymptotic properties (Ghosal et al., 1999, 2007, 2001; Walker et al., 2007; Shen et al., 2013).

A disadvantage of (2) is inefficient posterior computation, particularly as n increases. This has motivated a literature on faster approaches, including sequential approximations (Wang and Dunson, 2011; Zhang et al., 2014) and variational Bayes (Blei and Jordan, 2006). These methods are order dependent, tend to converge to local modes, and/or lack theory

support. [Newton and Zhang \(1999\)](#); [Newton \(2002\)](#) instead rely on predictive recursion. Such estimators are fast to compute and have theory support, but are also order dependent and do not provide a characterization of uncertainty. Alternatively, one can use a Polya tree as a conjugate prior ([Lavine, 1992, 1994](#)), and there is a rich literature on related multiscale and recursive partitioning approaches, such as the optional Polya tree ([Wong and Ma, 2010](#)). However, Polya trees have disadvantages in terms of sensitivity to a base partition and a tendency to favor spiky/erratic densities. These disadvantages are inherited by most of the computationally fast modifications.

Our proposed nearest neighbor-Dirichlet process has substantial advantages over current competitors. The basic idea is to rely on fast nearest neighbor search algorithms to group the data into local neighborhoods, and then condition on these neighborhoods in defining a Bayesian mixture model-based approach.

2 Methodology

2.1 Nearest Neighbor Dirichlet Process Framework

Let $d(x_1, x_2)$ denote a distance metric between data points $x_1, x_2 \in \mathcal{X}$. For $\mathcal{X} = \mathbb{R}^p$, the Euclidean distance is typically chosen. For each $i \in \{1, 2, \dots, n\}$, let $X_{i[j]}$ denote the j th nearest neighbor to X_i in the data $\mathcal{X}^{(n)} = (X_1, \dots, X_n)$, such that $d(X_i, X_{i[1]}) \leq \dots \leq d(X_i, X_{i[n]})$, with ties broken by increasing order of indices. The indices on the k nearest neighbors to X_i are denoted as $\mathcal{N}_i = \{j : d(X_i, X_j) \leq d(X_i, X_{i[k]})\}$, where by convention we define $X_{i[1]} = X_i$, for $i = 1, \dots, n$.

Fixing $x \in \mathcal{X}$, we model the density of the data within the i th neighborhood using

$$f_i(x) = \mathcal{K}(x; \theta_i), \quad \theta_i \sim P_0, \quad (3)$$

where θ_i are parameters specific to neighborhood i that are given a common prior distribution P_0 . The resulting posterior distribution of θ_i given data $\mathcal{X}^{(n)}$ and prior P_0 is

$$(\theta_i \mid \mathcal{X}^{(n)}, P_0) \sim P_0(\theta_i) \prod_{j \in \mathcal{N}_i} \mathcal{K}(X_j; \theta_i). \quad (4)$$

This posterior is in a simple analytic form if P_0 is conjugate to $\mathcal{K}(x; \theta)$. The prior P_0 can involve unknown parameters and borrows information across neighborhoods; this reduces the large variance problem common to nearest neighbor estimators. Refer to the examples later in the paper.

To combine the $f_i(x)$ s into a single global $f(x)$, similarly to equations (1)-(2), we let

$$f(x) = \sum_{i=1}^n \pi_i \mathcal{K}(x; \theta_i), \quad \pi = (\pi_i)_{i=1}^n \sim \text{Dirichlet}(\alpha, \dots, \alpha), \quad \theta_i \sim P_0. \quad (5)$$

Here, there are two main differences with Dirichlet process mixture models. First, we use k -nearest neighbors to allocate data to local neighborhoods instead of allowing that allocation to be unknown. Second, we use an n -dimensional symmetric Dirichlet density for the weights instead of a stick-breaking process; it is common to approximate (2) using a finite Dirichlet motivated by the result of Ishwaran and Zarepour (2002).

In usual mixture models that choose a Dirichlet prior for the weights π , one obtains a conjugate conditional posterior for π given latent variables indexing which component each data point is drawn from. Such conjugacy leads to a straightforward data augmentation Gibbs sampler, providing a routine approach for posterior computation in mixture models. Unfortunately, this and other samplers that rely on updating the allocation of data points to components tend to have famously poor performance as n increases. In our proposed approach, we avoid the need for Markov chain Monte Carlo by using nearest neighbor algorithms to allocate samples to clusters, defining a pseudo-posterior conditionally on the neighborhood structure.

Since the neighborhoods are overlapping, the conditional posterior for π under (5) is not exactly Dirichlet. However, since the radius of each neighborhood approaches zero as n increases (Biau and Devroye, 2015, Chapter 2), overlap becomes more and more minor, motivating the pseudo-posterior:

$$(\pi \mid \mathcal{X}^{(n)}) \sim \text{Dirichlet}(\alpha + 1, \dots, \alpha + 1). \quad (6)$$

This distribution is centered on $(1/n, \dots, 1/n)$ with concentration parameter $n(\alpha + 1)$. In practice, α is typically chosen to be close to zero and we let $k = k_n$ increase slowly with the sample size. Section 3 provides a theoretical justification for this choice of pseudo-posterior.

Based on equations (3)-(6), our nearest neighbor-Dirichlet process produces a pseudo-posterior distribution for the unknown density $f(x)$ through simple distributions for the parameters characterizing the density within each neighborhood and for the weights. To generate independent Monte Carlo samples from the pseudo-posterior for f , one can simply draw samples from (4) and (6) independently and plug these samples into (5). Although this is not exactly a coherent fully Bayesian posterior distribution, we claim that it can be used as a simple alternative to such a posterior in practice. This claim is backed up by theoretical arguments, simulation studies and a real data application in the sequel.

2.2 Illustration with Gaussian Kernels

Suppose we have independent and identically distributed observations $\mathcal{X}^{(n)}$ from the density f , where $X_i \in \mathbb{R}^p$ for $i = 1, \dots, n$ and f is an unknown density function with respect to the Lebesgue measure on \mathbb{R}^p for $p \geq 1$. Let $\mathbb{R}_+^{p \times p}$ denote the set of all real-valued $p \times p$ positive definite matrices. Fix $x \in \mathbb{R}^p$. We will illustrate the method for a general $p \geq 1$ and note key changes for the special case $p = 1$. We proceed by setting $\mathcal{K}(x; \theta)$ to be the multivariate Gaussian density $\phi_p(x; \eta, \Sigma) = (2\pi)^{-p/2} |\Sigma|^{-1/2} \exp\{-(x - \eta)^\top \Sigma^{-1} (x - \eta)/2\}$, where $\theta = (\eta, \Sigma)$, $\eta \in \mathbb{R}^p$ and $\Sigma \in \mathbb{R}_+^{p \times p}$. We first compute the neighborhoods \mathcal{N}_i corresponding to X_i as in Section 2.1 and place a normal-inverse Wishart prior on $\theta_i = (\eta_i, \Sigma_i)$, given by $(\eta_i, \Sigma_i) \sim \text{NIW}_p(\mu_0, \Sigma_i/\nu_0, \gamma_0, \Psi_0)$ independently for $i = 1, \dots, n$. That is, $\eta_i \mid \Sigma_i \sim \text{N}(\mu_0, \Sigma_i/\nu_0)$ and $\Sigma_i \sim \text{IW}_p(\gamma_0, \Psi_0)$ with $\mu_0 \in \mathbb{R}^p$, $\nu_0 > 0$, $\gamma_0 > p - 1$ and $\Psi_0 \in \mathbb{R}_+^{p \times p}$; for details about parametrization see Section H of the Appendix.

For $p = 1$, we have a univariate Gaussian density $\phi(x; \eta_i, \sigma_i^2)$ in neighborhood i with normal-inverse gamma priors $(\eta_i, \sigma_i^2) \sim \text{NIG}(\mu_0, \sigma_i^2/\nu_0, \gamma_0/2, \gamma_0\delta_0^2/2)$ independently for $i = 1, \dots, n$, with $\mu_0 \in \mathbb{R}$ and $\nu_0, \gamma_0, \delta_0^2 > 0$. That is, $\eta_i \mid \sigma_i^2 \sim \text{N}(\mu_0, \sigma_i^2/\nu_0)$ and $\sigma_i^2 \sim \text{IG}(\gamma_0/2, \gamma_0\delta_0^2/2)$. When $p = 1$, the $\text{IW}_p(\gamma_0, \Psi_0)$ density simplifies to an $\text{IG}(\gamma_0/2, \gamma_0\delta_0^2/2)$ density with $\delta_0^2 = \Psi_0/\gamma_0$.

Monte Carlo samples from the pseudo-posterior of $f(x)$ given the data $\mathcal{X}^{(n)}$ can be obtained using Algorithm 1. The corresponding steps for the univariate case are provided in Section G of the Appendix. Although the pseudo-posterior distribution of $f(x)$ lacks an

Algorithm 1: Nearest neighbor-Dirichlet process algorithm to obtain Monte Carlo samples from the pseudo-posterior of $f(x)$ given multivariate data $\mathcal{X}^{(n)}$ with Gaussian kernel and normal-inverse Wishart prior.

- **Step 1:** Compute the neighborhood \mathcal{N}_i for data point $X_i \in \mathbb{R}^p$ according to distance $d(\cdot, \cdot)$ with $(k - 1)$ nearest neighbors.
- **Step 2:** Update the parameters for neighborhood \mathcal{N}_i to $(\mu_i, \nu_n, \gamma_n, \Psi_i)$, where $\nu_n = \nu_0 + k$, $\gamma_n = \gamma_0 + k$, $\mu_i = \nu_n^{-1}(\nu_0\mu_0 + k\bar{X}_i)$, $\bar{X}_i = k^{-1} \sum_{j \in \mathcal{N}_i} X_j$ and $\Psi_i = \Psi_0 + \sum_{j \in \mathcal{N}_i} (X_j - \bar{X}_i)(X_j - \bar{X}_i)^\top + k\nu_0\nu_n^{-1}(\bar{X}_i - \mu_0)(\bar{X}_i - \mu_0)^\top$.
- **Step 3:** To compute the t th Monte Carlo sample $f^{(t)}(x)$ of $f(x)$, sample Dirichlet weights $\pi^{(t)} \sim \text{Dirichlet}(\alpha + 1, \dots, \alpha + 1)$ and neighborhood specific parameters $(\eta_i^{(t)}, \Sigma_i^{(t)}) \sim \text{NIW}_p(\mu_i, \Sigma_i^{(t)}/\nu_n, \gamma_n, \Psi_i)$, independently for $i = 1, \dots, n$, and set

$$f^{(t)}(x) = \sum_{i=1}^n \pi_i^{(t)} \phi_p(x; \eta_i^{(t)}, \Sigma_i^{(t)}). \quad (7)$$

analytic form, we can obtain a simple form for its pseudo-posterior mean by integrating

over the pseudo-posterior distribution of $(\theta_i)_{i=1}^n$ and π . Recall the definitions of μ_i and Ψ_i from Step 2 of Algorithm 1 and define $\Lambda_i = \{\nu_n(\gamma_n - p + 1)\}^{-1}(\nu_n + 1)\Psi_i$. Then the pseudo-posterior mean of $f(x)$ is given by

$$\hat{f}_n(x) = \frac{1}{n} \sum_{i=1}^n t_{\gamma_n - p + 1}(x; \mu_i, \Lambda_i). \quad (8)$$

Here $t_\gamma(x; \mu, \Lambda) = [\Gamma\{(\gamma + p)/2\}/\Gamma(\gamma/2)] (\gamma\pi)^{-p/2} |\Lambda|^{-1/2} [1 + (x - \mu)^\top (\gamma\Lambda)^{-1} (x - \mu)]^{-(\gamma+p)/2}$ for $x \in \mathbb{R}^p$ is the p -dimensional Student's t-density with degrees of freedom $\gamma > 0$, location $\mu \in \mathbb{R}^p$ and scale matrix $\Lambda \in \mathbb{R}_+^{p \times p}$. For the univariate case, we have γ_n and ν_n as in Algorithm 1. The pseudo-posterior mean of $f(x)$ is given by

$$\hat{f}_n(x) = \frac{1}{n} \sum_{i=1}^n \frac{1}{\lambda_i} t_{\gamma_n} \left(\frac{x - \mu_i}{\lambda_i} \right), \quad (9)$$

where $\mu_i = \nu_0 \nu_n^{-1} \mu_0 + k \nu_n^{-1} \bar{X}_i$, $\bar{X}_i = k^{-1} \sum_{j \in \mathcal{N}_i} X_j$, $\lambda_i = \delta_i \{(\nu_n + 1)/\nu_n\}^{1/2}$, $\delta_i^2 = \gamma_n^{-1} \{\gamma_0 \delta_0^2 + \sum_{j \in \mathcal{N}_i} (X_j - \bar{X}_i)^2 + k \nu_0 \nu_n^{-1} (\mu_0 - \bar{X}_i)^2\}$. Here $t_{\gamma_n}(\cdot)$ represents the univariate Student's t-density with γ_n degrees of freedom.

2.3 Cross-validation for Hyperparameter Choice

The hyperparameters in the prior for the neighborhood-specific parameters need to be chosen carefully - we found results to be sensitive to γ_0 and Ψ_0 . If non-informative values are chosen for these key hyperparameters, we tend to inherit typical problems of nearest neighbor estimators including lack of smoothness and high variance. Suppose $\Sigma \sim \text{IW}_p(\gamma_0, \Psi_0)$ and for $i, j = 1, \dots, p$, let Σ_{ij} and $\Psi_{0,ij}$ denote the i, j th entry of Σ and Ψ_0 , respectively. Then $\Sigma_{jj} \sim \text{IG}(\gamma_*/2, \Psi_{0,jj}/2)$ where $\gamma_* = \gamma_0 - p + 1$. Thus borrowing from the univariate case, we set $\Psi_{0,jj} = \gamma_* \delta_0^2$ and $\Psi_{0,ij} = 0$ for all $i \neq j$, which implies that $\Psi_0 = (\gamma_* \delta_0^2) I_p$ and we use leave-one-out cross validation to select the optimum δ_0^2 . With p dimensional data, we recommend fixing $\gamma_0 = p$ which implies a multivariate Cauchy prior predictive density. We choose the leave-one-out log likelihood as the criterion function for cross-validation, which is closely related to minimizing the Kullback-Leibler divergence between the true and estimated density (Hall, 1987; Bowman, 1984). The explicit expression for the pseudo-posterior mean in equations (8) and (9) makes cross-validation computationally efficient. The description of a fast implementation is provided in Section F of the Appendix.

The proposed method has substantially faster runtime if one bypasses cross-validation and uses a default set of choices of hyperparameters before initiating Monte Carlo sampling. Refer to Section 4.1 for the default choices.

3 Theory

3.1 Asymptotic Properties

There is a rich literature on asymptotic properties of the exact posterior for an unknown density under Dirichlet process mixtures; refer, for example to Ghosal et al. (1999), Ghosal et al. (2007). Unfortunately, the tools used for studying frequentist asymptotic properties of Bayesian posteriors do not apply to the pseudo-posterior produced by the nearest neighbor-Dirichlet process. Hence, completely new tools need to be developed, which is highly non-trivial in this case.

We focus on proving pointwise consistency of the pseudo-posterior of $f(x)$ induced by (3)-(6) for each $x \in [0, 1]^p$, considering the Gaussian kernel as illustrated in Section 2.2 for our purposes. This is established by separately considering the mean and variance of the pseudo-posterior distribution, that is, we first show that the pseudo-posterior mean defined in (8) is pointwise consistent and then show that the pseudo-posterior variance vanishes asymptotically. The key idea behind our proofs is to show that the pseudo-posterior mean is asymptotically close to a kernel density estimator with suitably chosen bandwidth for fixed p and $k = k_n \rightarrow \infty$ at a desired rate. The proof then follows from standard arguments leading to consistency of kernel density estimators. We note here that the proposed pseudo-posterior mean mimics a kernel density estimator only in the asymptotic regime; in finite sample simulation studies as can be seen in Section 4, the proposed method has much improved performance. The detailed proofs of all results in this section are in the Appendix.

Consider independent and identically distributed data $\mathcal{X}^{(n)}$ from a fixed unknown density f_0 with respect to the Lebesgue measure on \mathbb{R}^p equipped with the Euclidean metric, inducing the measure P_{f_0} on $\mathcal{B}(\mathbb{R}^p)$. Hereby, we will use $E\{f(x) \mid \mathcal{X}^{(n)}\}$, $\text{var}\{f(x) \mid \mathcal{X}^{(n)}\}$ and $\text{pr}\{f(x) \in B \mid \mathcal{X}^{(n)}\}$ to denote the mean of $f(x)$, variance of $f(x)$ and probability of the event $\{f(x) \in B\}$ for $B \in \mathcal{B}(\mathbb{R}^p)$, respectively, under the pseudo-posterior distribution of $f(x)$ implied by equations (3)-(6). We make the following regularity assumptions on f_0 :

Assumption 3.1 (Support). f_0 is compactly supported on $[0, 1]^p$.

Assumption 3.2 (Bounded curvature). f_0 is continuous on $[0, 1]^p$ with $\|\nabla f_0(x)\|_2 \leq L$ for all $x \in [0, 1]^p$ and some finite $L > 0$.

Assumption 3.3 (Bounded sup-norm). $\|\log(f_0)\|_\infty < \infty$.

Assumptions 3.1 and 3.2 (Evans et al., 2002) are common in the nearest neighbor literature, and ensure that the underlying true density f_0 is smooth enough for our purposes. Assumption 3.3 (Rivoirard and Rousseau, 2012) is standard in the Bayesian nonparametric literature. For $i = 1, \dots, n$, recall the definitions of μ_i and Λ_i from (8):

$$\mu_i = \frac{\nu_0}{\nu_n} \mu_0 + \frac{k}{\nu_n} \bar{X}_i, \quad \Lambda_i = \frac{\nu_n + 1}{\nu_n(\gamma_n - p + 1)} \Psi_i.$$

Define the bandwidth matrix $H = H_n = h_n^2 I_p$ where $h_n^2 = \{\nu_n(\gamma_n - p + 1)\}^{-1}(\nu_n + 1)(\gamma_0 - p + 1) \delta_0^2$. Fix $x \in [0, 1]^p$. To prove the consistency of the posterior mean, we first show that $\hat{f}_n(x)$ and $f_K(x) = (1/n) \sum_{i=1}^n t_{\gamma_n - p + 1}(x; X_i, H_n)$ are asymptotically close, that is we show that $E_{P_{f_0}}(|\hat{f}_n(x) - f_K(x)|) \rightarrow 0$ as $n \rightarrow \infty$. To obtain this result, we approximate μ_i by X_i and Λ_i by H_n using successive applications of the mean value theorem. Finally, we exploit the convergence of $f_K(x)$ to the true value $f_0(x)$ to obtain the consistency of $\hat{f}_n(x)$. The proof of convergence of $f_K(x)$ to $f_0(x)$ is provided in Section E of the Appendix. The precise statement regarding the consistency of the pseudo-posterior mean is given in the following theorem. Let $a \wedge b$ denote the minimum of a and b .

Theorem 3.4. *Fix $x \in [0, 1]^p$. Let $k = o(n^{i_0})$ with $i_0 = \{2/(p^2 + p + 2)\} \wedge \{4/(p + 2)^2\}$ such that $k \rightarrow \infty$ as $n \rightarrow \infty$, and $\nu_0 = o\{n^{-2/p} k^{(2/p)+1}\}$. Then, $\hat{f}_n(x) \rightarrow f_0(x)$ in P_{f_0} -probability as $n \rightarrow \infty$.*

We now look at the pseudo-posterior variance of $f(x)$. In equation (6), we let $\omega = \alpha + 1$,

$$R_n = \frac{\Gamma\{(\gamma_n - p + 2)/2\}}{\Gamma\{(\gamma_n - p + 1)/2\}} \left[\frac{\nu_n + 2}{4\pi\nu_n(\gamma_n - p + 2)} \right]^{p/2},$$

and $D_n = \{2(\gamma_n - p + 2)(\nu_n + 1)\}^{-1}(\gamma_n - p + 1)(\nu_n + 2) \rightarrow 1/2$ as $n \rightarrow \infty$. For $i = 1, \dots, n$, let $B_i = D_n \Lambda_i$ and define $\hat{f}_{var}(x) = (1/n) \sum_{i=1}^n t_{\gamma_n - p + 2}(x; \mu_i, B_i)$. As $n \rightarrow \infty$, analogous steps to the ones used in the proof of Theorem 3.4 can be used to imply that $\hat{f}_{var}(x) \rightarrow f_0(x)$ in P_{f_0} -probability. Also, as $n \rightarrow \infty$ by Stirling's approximation, $k^{(p-1)/2} R_n \rightarrow (4\pi)^{-1/2}$. Finally, let $a_n(x) = R_n D_n^{-p/2} \hat{f}_{var}(x)$. We now provide an upper bound on the pseudo-posterior variance of $f(x)$ which shows convergence of the pseudo-posterior variance to 0 as $n \rightarrow \infty$.

Theorem 3.5. *Under Assumptions 3.1-3.3 with x, k and ν_0 as in Theorem 3.4, we have*

$$\text{var}\{f(x) \mid \mathcal{X}^{(n)}\} \leq \frac{a_n(x)}{|H_n|^{1/2}} \left\{ \frac{1}{(n\omega + 1)} + \frac{1}{n} \right\}. \quad (10)$$

In particular, $\text{var}\{f(x) \mid \mathcal{X}^{(n)}\} \rightarrow 0$ in P_{f_0} -probability as $n \rightarrow \infty$.

Refer to Sections B and C in the Appendix for proofs of Theorems 4 and 5, respectively. Pointwise pseudo-posterior consistency follows directly from Theorem 3.4 and 3.5 as shown below.

Theorem 3.6. *Let Assumption 3.1 be satisfied with x, k and ν_0 as in Theorem 3.4. Fix $\epsilon > 0$ and define the ϵ -ball around $f_0(x)$ by $U_\epsilon = \{y_* : |y_* - f_0(x)| \leq \epsilon\}$. Then, $\text{pr}\{f(x) \in U_\epsilon \mid \mathcal{X}^{(n)}\} \rightarrow 0$ in P_{f_0} -probability as $n \rightarrow \infty$.*

Proof. Fix $\epsilon > 0$ and consider the ϵ -ball $U_\epsilon = \{y_* : |y_* - f_0(x)| \leq \epsilon\}$. Then by Chebychev's inequality, we have $\text{pr}\{f(x) \in U_\epsilon \mid \mathcal{X}^{(n)}\} \leq [\{\hat{f}_n(x) - f_0(x)\}^2 + \text{var}\{f(x) \mid \mathcal{X}^{(n)}\}]/\epsilon^2 \rightarrow 0$ in P_{f_0} -probability as $n \rightarrow \infty$, using Theorems 3.4 and 3.5. \square

3.2 Choice of Dirichlet Prior Parameter

Although Theorem 3.6 implies consistency of the pseudo-posterior for fixed x and any α , the choice of α impacts frequentist coverage of the pseudo-posterior credible intervals as it directly influences the pseudo-posterior variance of $f(x)$ through Theorem 3.5. We now describe a data-dependent method to choose α using Bernstein-von Mises results for linear functionals of Bayesian density estimators in the univariate setup (Rivoirard and Rousseau, 2012). The key idea we adopt is to consider a relevant functional of the density such as its mean, obtain its Bernstein-von Mises limit distribution using the result in Rivoirard and Rousseau (2012) and equate the variance of this limit distribution with the variance of the relevant functional of the NN-DP density estimator in the asymptotic setting.

Following Rivoirard and Rousseau (2012), let $\mathcal{P}(f) = \int \tilde{p}(u)f(u) du$ for a density f on \mathfrak{R} . Suppose X_1, \dots, X_n are independent and identically distributed data from a compactly supported density f_0 , where \tilde{p} and f_0 satisfy conditions in Rivoirard and Rousseau (2012). Define $q(u) = \tilde{p}(u) - \int \tilde{p}(v)f_0(v) dv$ and let \mathcal{F}_n be the empirical distribution function of X_1, \dots, X_n . Then under a suitable prior distribution on $f(\cdot)$, Rivoirard and Rousseau (2012) show that the posterior distribution of $n^{1/2}\{\mathcal{P}(f) - \mathcal{P}(\mathcal{F}_n)\}$ with $\mathcal{P}(\mathcal{F}_n) = n^{-1} \sum_{i=1}^n \tilde{p}(X_i)$ is asymptotically Gaussian with mean 0 and variance $\Omega_0 = \int q^2(x)f_0(x) dx$.

As a specific example, consider the case when $\tilde{p}(u) = u$, corresponding to the mean of the density. Then, we have $\Omega_0 = \int (u - m_{f_0})^2 f_0(u) du = \sigma_{f_0}^2$ where $m_{f_0} = \int u f_0(u) du$ and $\sigma_{f_0}^2$ is the population variance of f_0 . Our strategy for finding a value of α when f has the nearest neighbor-Dirichlet process formulation involves equating the pseudo-posterior variance of $n^{1/2}\mathcal{P}(f)$ with $\sigma_{f_0}^2$ as $n \rightarrow \infty$. When f has the nearest neighbor-Dirichlet process formulation, $\mathcal{P}(f) = \int u f(u) du = \sum_{i=1}^n \pi_i \eta_i$, following from Section 2.2. The variance of $n^{1/2}\mathcal{P}(f)$ when f has the nearest neighbor-Dirichlet process formulation is provided below.

Theorem 3.7. *Suppose f_0 satisfies Assumptions 3.1-3.3 with $p = 1$. Let f have the nearest neighbor-Dirichlet process formulation, and k, ν_0 be chosen as in Theorem 3.4. Let $\Theta = \int u f(u) du = \sum_{i=1}^n \pi_i \eta_i$ as in Section 2.2. For $\gamma_n > 2$, define $v_i = \{(\nu_n + 1)(\gamma_n - 2)\}^{-1} \gamma_n \lambda_i^2$ for $i = 1, \dots, n$, $\bar{v} = n^{-1} \sum_{i=1}^n v_i$, $\bar{\mu} = n^{-1} \sum_{i=1}^n \mu_i$ and $S_\mu^2 = n^{-1} \sum_{i=1}^n (\mu_i - \bar{\mu})^2$. Then*

$$\text{var}(n^{1/2}\Theta \mid \mathcal{X}^{(n)}) = \bar{v} + \frac{nS_\mu^2 + (n-1)\bar{v}}{n\omega + 1}.$$

Equating the above with $\sigma_{f_0}^2$ and letting $n \rightarrow \infty$, we get the following choice of α given

by:

$$\alpha = \frac{\gamma_0 \delta_0^2}{\sigma_{f_0}^2 \gamma_n \nu_n}. \quad (11)$$

The proof of Theorem 3.7 and derivation of (11) are in Section D of the Appendix. Due to the lack of a multivariate analogue of the result discussed in Rivoirard and Rousseau (2012), a multivariate analogue of the choice of α is not immediate. Let H_n be as defined in Section 3.1 and Σ_{f_0} be the unknown population covariance matrix of f_0 . Then, one may generalize the findings of (11) to a multivariate extension given by $\alpha = \nu_n^{-1} |H_n \Sigma_{f_0}^{-1}|$. Once δ_0^2 is estimated according to Section 2.3 and the underlying population variance is estimated, one can use (11) or its multivariate analogue to select an appropriate value of α .

4 Simulation Experiments

4.1 Preliminaries

In this section, we compare the performance of the proposed density estimator with several other standard density estimators through several numerical experiments. We evaluate performance based on the expected \mathcal{L}_1 distance (Devroye and Györfi, 1985). For the pair (f_0, \hat{f}) , where f_0 is the true data generating density and \hat{f} is an estimator, the expected \mathcal{L}_1 distance is defined as $\mathcal{L}_1(f_0, \hat{f}) = E_{P_{f_0}} \{ \int |f_0(x) - \hat{f}(x)| dx \}$. Given a sample size n , we compute an estimate $\hat{\mathcal{L}}_1(f_0, \hat{f})$ of $\mathcal{L}_1(f_0, \hat{f})$ in two steps. First, we sample $X_1, \dots, X_n \sim f_0$ and obtain \hat{f} based on this sample, and then further sample n_t independent test points $X_{n+1}, \dots, X_{n+n_t} \sim f_0$ and compute

$$\hat{L} = \frac{1}{n_t} \sum_{i=1}^{n_t} \left| \frac{\hat{f}(X_{n+i})}{f_0(X_{n+i})} - 1 \right|.$$

In the second step, to approximate the expectation with respect to P_{f_0} , the first step is repeated R times. Letting \hat{L}_r denote the estimate for the r th replicate, we compute the final estimate as $\hat{\mathcal{L}}_1(f_0, \hat{f}) = (1/R) \sum_{r=1}^R \hat{L}_r$. Then, it follows that $\hat{\mathcal{L}}_1(f_0, \hat{f}) \rightarrow \mathcal{L}_1(f_0, \hat{f})$ as $n_t, R \rightarrow \infty$, by the law of large numbers. In our experiments, we set $n_t = 500$ and $R = 20$. Lastly, let 0_p and 1_p denote the vector of all 0s and 1s in \mathbb{R}^p for $p \geq 1$.

All simulations were carried out using the R programming language (R Core Team, 2018). For Dirichlet process mixture models, we collect 1,000 Markov chain Monte Carlo (MCMC) samples after discarding a burn-in of 1,500 samples using the `dirichletprocess` package (J. Ross and Markwick, 2019) with default choices of prior hyperparameters. For the nearest neighbor-Dirichlet process, 1,000 Monte Carlo samples are taken. For the kernel density estimator, we select the bandwidth by the default plug-in method `hpi` for univariate cases

and Hpi for multivariate cases (Sheather and Jones, 1991; Wand and Jones, 1994) using the package `ks` (Duong, 2020). We additionally consider the k-nearest neighbor estimator studied in Mack and Rosenblatt (1979), setting the number of neighbors $k = n^{1/2}$, and the variational Bayes (VB) approximation to Dirichlet process mixture models (Blei and Jordan, 2006) in all of our numerical studies. We consider the recursive predictive density estimator (RD) from Hahn et al. (2018) and Polya tree mixtures (PTM) using the package `DPpackage` (Jara et al., 2011) for univariate data. Dirichlet process mixture model hyperparameter values are kept the same in both the MCMC and variational Bayes implementations, with the number of components of the variational family set to 10 for all cases. We denote the nearest neighbor-Dirichlet process, Dirichlet process mixture (DPM) implemented with MCMC, kernel density estimator, variational Bayes approximation to the DPM, and k-nearest neighbor density estimator by NN-DP, DP-MC, KDE, DP-VB and KNN, respectively, in tables and figures.

One might choose to avoid cross-validation in order to gain computational efficiency while using the NN-DP. Following Section 2.3, the default values $\mu_0 = 0_p$, $\nu_0 = 0.001$, $\gamma_0 = p$, and $\Psi_0 = I_p$ were observed to work well in the simulations and applications that we carried out.

4.2 Univariate Cases

We set $n = 200, 500$ with $k_n = \lfloor n^{1/3} \rfloor + 1$ where $\lfloor n_0 \rfloor$ denotes the greatest integer less than or equal to n_0 . We consider 10 choices of f_0 from the R package `benchden` (Mildenberger and Weinert, 2012); the specific choices are Cauchy (CA), claw (CW), double exponential (DE), Gaussian (GS), inverse exponential (IE), lognormal (LN), logistic (LO), skewed bimodal (SB), symmetric Pareto (SP), and sawtooth (ST) with default choices of the corresponding parameters. The prior hyperparameter choices for the proposed method are $\mu_0 = 0$, $\nu_0 = 0.001$, $\gamma_0 = 1$; δ_0^2 is chosen via the cross-validation method of Section 2.3. In Figure 1, we plot the estimated \mathcal{L}_1 errors for the 10 densities listed above; the corresponding data are given in Table 3 in Section I of the Appendix. Results of KNN are omitted in Figure 1 due to higher values compared to other methods. For the kernel density estimator and recursive predictive density estimator, the plot and the table exclude the results for CA, IE and SP due to very high \mathcal{L}_1 errors.

In general, the kernel density estimator and recursive predictive density estimator struggle when data are generated from a heavy-tailed distribution so much that we have to omit results for some of the cases in Table 3. For instance, when $n = 500$ and f_0 is the standard Cauchy (CA) density, the estimated \mathcal{L}_1 error we obtain for the KDE is 38501.85 and the algorithm for the recursive density estimate did not converge. For very spiky multi-modal densities, such as the claw (CW) and sawtooth (ST), both the kernel density estimator and the MCMC and VB implementations of the DPM struggle. The k-nearest neighbor estimate has comparably high \mathcal{L}_1 error across all the cases considered. The NN-DP pseudo-

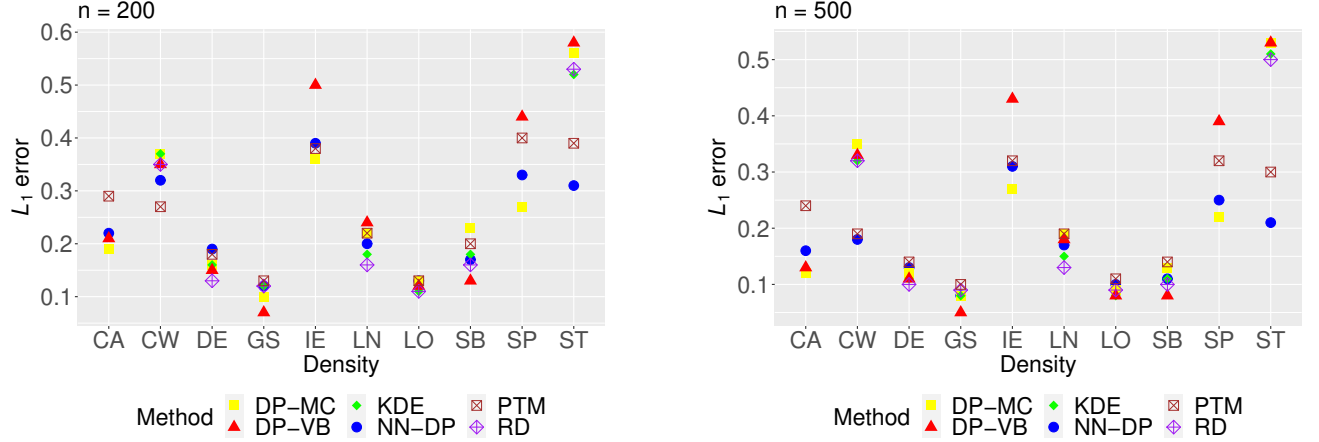


Figure 1: Scatter plot of $\hat{\mathcal{L}}_1(f_0, \hat{f})$ for the 10 different choices of the true density f_0 and different estimators \hat{f} for univariate data.

posterior mean \hat{f}_n performs well across all the settings considered in Table 3, seemingly achieving the best of both worlds; comparable in accuracy with the MCMC implementation of DPMS for heavy-tailed densities and with the kernel density estimator or variational Bayes approximation for smooth densities. Moreover, the NN-DP and PTM exhibit superior performance to all competitors in very spiky multi-modal cases, while the NN-DP does better in the heavy-tailed cases.

In Figure 2, we show the performance of the proposed pseudo-posterior mean estimate \hat{f}_n along with the posterior mean under the MCMC implementation of the Dirichlet process mixture model with 500 samples generated from the sawtooth (ST) density. The Dirichlet process mixture is unable to detect the multiple spikes, merging adjacent modes to form larger clusters, perhaps due to inadequate mixing of the Markov chain Monte Carlo sampler or to the Gaussian kernels used in the mixture. The nearest neighbor-Dirichlet process has dramatically better performance. We also compare the performance of the two methods with a smoother test density in Figure 3, where the data are generated from a skewed bimodal (SB) distribution. Both the estimates are comparable, but the nearest neighbor-Dirichlet process provides better uncertainty quantification. Similar results are obtained for $n = 1000$, and hence are omitted.

4.3 Multivariate Cases

For the multivariate cases, we consider $n = 200$ and 1000 . The number of neighbors is set to $k = 10$ and the dimension p is chosen from $\{2, 3, 4, 6\}$. Recall the definition of $\phi_p(x; \mu, \Sigma)$ from Section 2.2 and let $\Phi(x)$ be the cumulative distribution function of the standard Gaussian density. Let $S_0 = \rho 1_p 1_p^T + (1 - \rho) I_p$ with $\rho = 0.8$. Let $x = (x_1, \dots, x_p)^T$. We consider

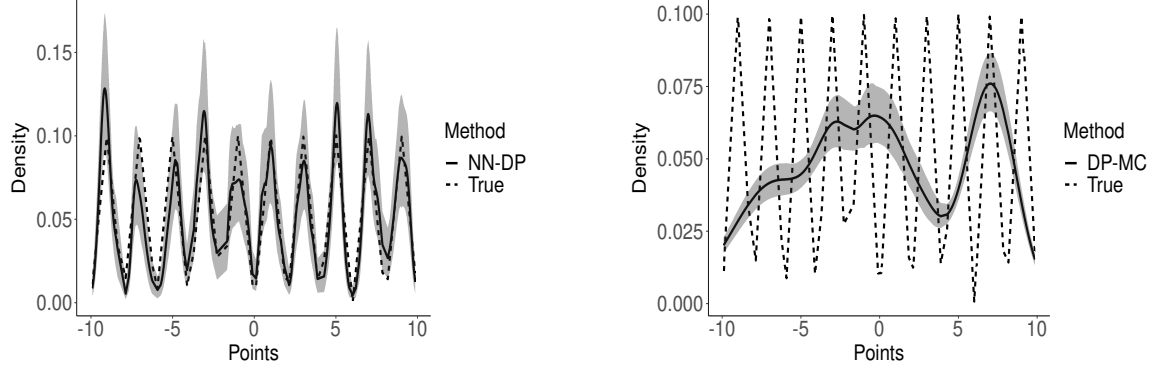


Figure 2: Plot comparing density estimates for the nearest neighbor-Dirichlet process and MCMC implementation of the Dirichlet process mixture for data of sample size $n = 500$ generated from the sawtooth (ST) density. Shaded regions correspond to 95% (pseudo) posterior credible intervals.

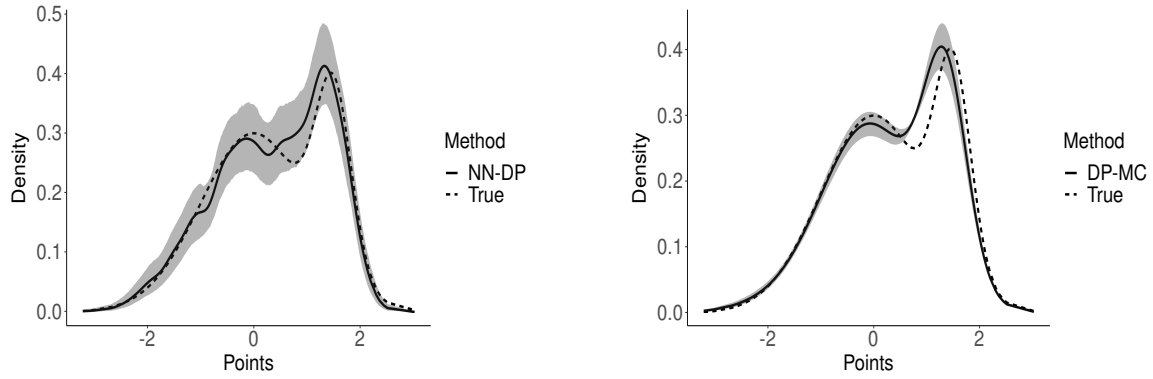


Figure 3: Similar to Figure 2, with data of sample size $n = 500$ generated from the skewed bimodal (SB) density.

the following cases.

- (1) *Mixture of Gaussians (MG)*: $f_0(x) = 0.4 \phi_p(x; m_1, S_0) + 0.6 \phi_p(x; m_2, S_0)$, where $m_1 = -2 \times 1_p, m_2 = 2 \times 1_p$.
- (2) *Skew normal (SN)*: $f_0(x) = 2\phi_p(x; m_0, S_0)\Phi\{s_0^T W^{-1}(x - m_0)\}$ (Azzalini, 2005), where W is the diagonal matrix with diagonal entries $W_{ii}^2 = S_{0,ii}$ for $i = 1, \dots, p$. We choose $m_0 = 0_p$ and the skewness parameter vector $s_0 = 0.5 \times 1_p$.
- (3) *Multivariate t-distribution (T)*: $f_0(x) = t_{d_0}(x; m_*, S_0)$ is the density of the p -dimensional multivariate Student's t-distribution as in Section 2.2. We set $d_0 = 10$ and $m_* = 1_p$.
- (4) *Mixture of multivariate skew t-distributions (MST)*: We consider a two component mixture of multivariate skew t-distribution (Azzalini, 2005) given by $f_0(x) = 0.25 t_{d_0}(x; m_1, S_0, s_0) + 0.75 t_{d_0}(x; m_2, S_0, s_0)$. Here, $t_d(\cdot; \mu, S, s)$ is the skew t-density with parameters d, μ, S, s , with d_0, s_0 defined as before and m_1, m_2 the same as in the first case.
- (5) *Multivariate Cauchy (MVC)*: $f_0(x) \propto \{1 + (x - \mu_*)^T S_0^{-1}(x - \mu_*)\}^{-1}$ where $\mu_* = 0_p$.
- (6) *Multivariate Gamma (MVG)*: $f_0(x) \propto c_\Phi(F_1(x_1), \dots, F_p(x_p) \mid S_0) \prod_{j=1}^p f_j(x_j; \gamma_{j1}, \gamma_{j2})$ where f_j and F_j denote the density and distribution function of the univariate gamma distribution with shape parameter γ_{j1} and rate parameter γ_{j2} , respectively, for $j = 1, \dots, p$ and $c_\Phi(\cdot \mid \Gamma)$ is as described in Song (2000). This is a Gaussian copula based construction of the multivariate gamma distribution. We set $\gamma_{j1} = \gamma_{j2} = 1$ for $j = 1, \dots, p$.

The hyperparameters for the nearest neighbor-Dirichlet process are chosen as $\mu_0 = 0_p, \nu_0 = 0.001, \gamma_0 = p$ and $\Psi_0 = \{(\gamma_0 - p + 1)\delta_0^2\}I_p = \delta_0^2 I_p$, where the optimal δ_0^2 is chosen via cross-validation as described in Section 2.3. Similar choices of hyperparameters are made for the MCMC and VB implementations of the DPM except for δ_0^2 , which was set to 1. We report the results in Figure 4 with the corresponding numerical values provided in Table 4 of Section I of the Appendix.

The \mathcal{L}_1 error of the nearest neighbor-Dirichlet process scales nicely with the dimension for all the cases considered as demonstrated in Figure 4. This is not the case for the MCMC and variational implementations of the DPM. In some cases, the Dirichlet process mixture shows a sudden increase in \mathcal{L}_1 error with increasing dimension. For example, with 200 samples drawn from the mixture of two Gaussians (MG), the \mathcal{L}_1 error for the DP-MC jumps from 0.20 to 0.53 when p increases from 2 to 3. The kernel density estimator shows a noticeably sharp decline in performance - when the dimension is changed from 2 to 6, the average increase in \mathcal{L}_1 error is by factors of about 5 and 7 for sample sizes 200 and 1000, respectively. The MCMC and variational implementations of the DPM perform slightly better than the NN-DP when the true density is unimodal, including for the skew-normal (SN) and multivariate t-distribution (T), while the DP-MC has inferior performance compared to the NN-DP for the discrete mixture cases. DP-VB suffers when the true density is multivariate gamma (MVG), and especially in the heavy-tailed case of multivariate Cauchy (MVC). Overall from

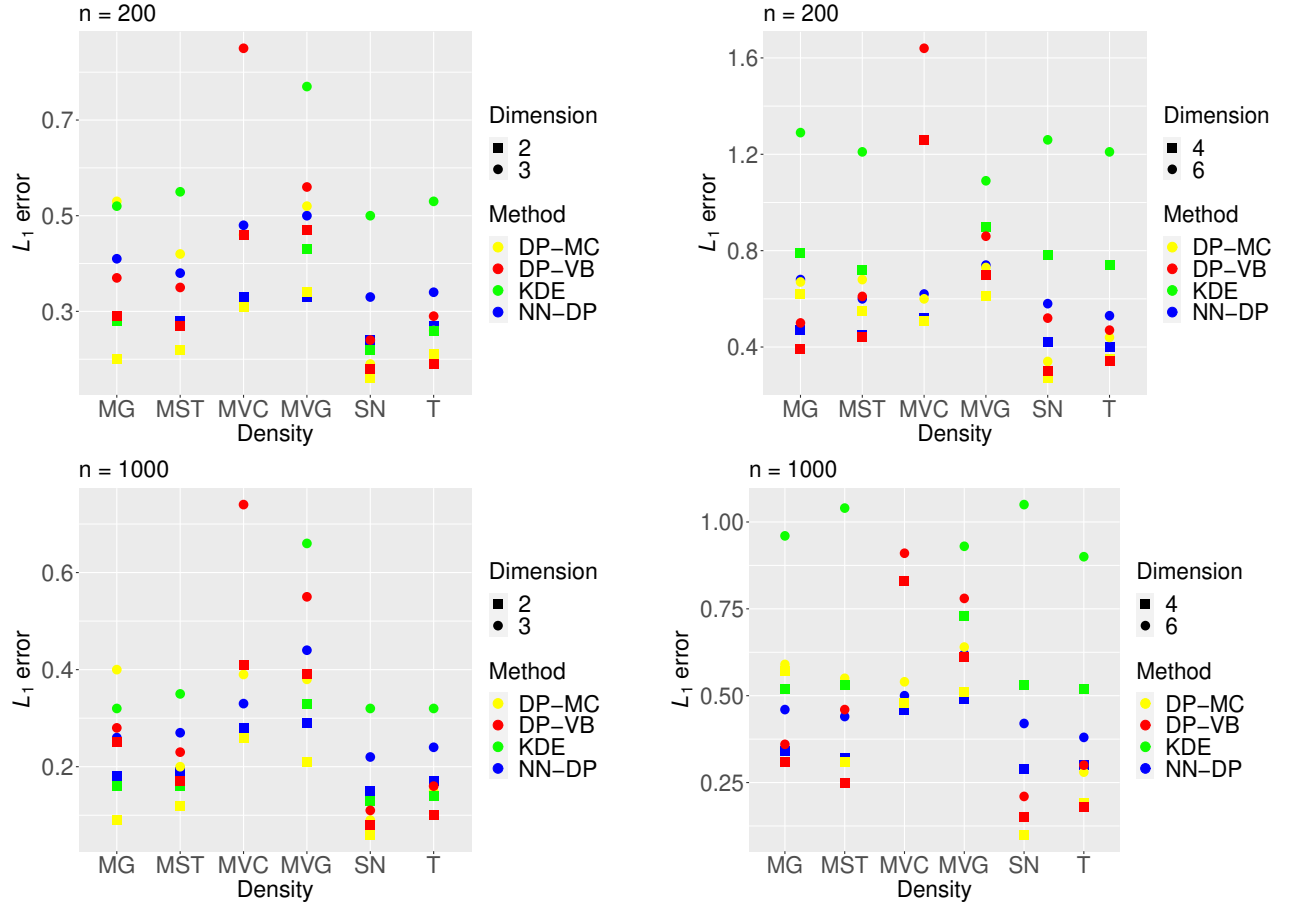


Figure 4: Scatter plot of $\hat{\mathcal{L}}_1(f_0, \hat{f})$ for the 6 different choices of the true density f_0 and different estimators \hat{f} for multivariate data.

Estimator	CA	CW	DE	GS	IE	LN	LO	SB	SP	ST
NN-DP	0.75	0.89	0.75	0.92	0.81	0.92	0.81	0.88	0.72	0.91
DP-MC	0.50	0.06	0.35	0.33	0.35	0.30	0.52	0.36	0.47	0.14
DP-VB	0.33	0.18	0.28	0.79	0.14	0.19	0.10	0.40	0.20	0.07

Table 1: Comparison of the frequentist coverage of 95% (pseudo) posterior credible intervals of the nearest neighbor-Dirichlet process and the MCMC and variational implementations of the Dirichlet process mixture for univariate data. Number of replications and sample size are $R_{cov} = 200$ and $n_{cov} = 500$, respectively.

Figure 4 the NN-DP has more consistent performance across a wide range of true density functions and dimensions.

4.4 Accuracy of Uncertainty Quantification

In this section, we assess frequentist coverage of 95% pseudo-posterior credible intervals for the NN-DP and compare with coverage based on the 95% posterior credible intervals obtained from DP-MC and DP-VB. We do not include frequentist coverage for Polya tree mixtures (PTMs) due to the lack of available code. We consider the cases $p \in \{1, 2\}$ in our experiments with sample size $n = 500$. For each choice of density f_0 , we fix $n_t = 200$ test points $\mathcal{X}_t = \{X_{t1}, \dots, X_{tn_t}\}$ generated from the density f_0 . With these fixed test points we generate $n = 500$ data points in our sample for $R_{cov} = 200$ times and check the coverage of posterior/pseudo-posterior credible intervals obtained from the three methods. We implement the DP-MC and DP-VB as before, while for the NN-DP we take $k = \lfloor 500^{1/3} \rfloor + 1 = 8$ in the univariate case, $k = 5$ in the bivariate case, α as in Section 3.2 and other hyperparameters chosen as before. In Table 1 and in Table 2, we report the average coverage probability across all the points in the test data \mathcal{X}_t for the univariate and bivariate cases, respectively.

For univariate densities, both the MCMC implementation of the DPM and variational Bayes approximation to the DPM display severe under-coverage. The NN-DP shows near nominal coverage in the smooth Gaussian (GS) and lognormal (LN) densities, while also attaining near nominal coverage in the skewed bimodal (SB), claw (CW) and sawtooth (ST) densities which are multi-modal. The shortcomings of DP-MC and DP-VB are noticeable when dealing with spiky densities such as the claw or sawtooth. For bivariate cases considered in Table 2 we see a similar trend; the NN-DP method provides uniformly better uncertainty quantification across all the densities considered.

Estimator	MG	MST	MVC	MVG	SN	T
NN-DP	0.92	0.88	0.66	0.80	0.92	0.88
DP-MC	0.44	0.31	0.35	0.24	0.08	0.17
DP-VB	0.56	0.58	0.18	0.55	0.49	0.57

Table 2: Comparison of the frequentist coverage of 95% (pseudo) posterior credible intervals of the nearest neighbor-Dirichlet process and the MCMC and variational implementations of the Dirichlet process mixture for bivariate data. Number of replications and sample size are $R_{cov} = 200$ and $n_{cov} = 500$, respectively.

4.5 Runtime Comparison

The results in the previous subsection suggest that the variational approximation to the DPM posterior has dramatic under-coverage with respect to the nominal frequentist coverage. Hence, the VB approach is not useful for uncertainty quantification. For this reason, we focus our comparison of runtimes on the NN-DP and the MCMC implementation of the DPM, noting that VB algorithms are faster than either of these approaches.

With n data points in p dimensions, the initial nearest neighbor allocation into n neighborhoods can be carried out in $\mathcal{O}(n \log n)$ steps (Vaidya, 1986; Ma and Li, 2019). Once the neighborhoods are determined with $k_n = k$ points in each neighborhood, obtaining the neighborhood specific empirical means and covariance matrices has $\mathcal{O}(nkp + nkp^2) = \mathcal{O}(nkp^2)$ complexity. Obtaining the pseudo-posterior mean (8) then requires inversion of n such $p \times p$ matrices to evaluate the multivariate t-density, with a runtime of $\mathcal{O}(np^3)$. Therefore, the total runtime to obtain the pseudo-posterior mean is of the order $\mathcal{O}(nkp^2 + np^3)$. When we are interested in uncertainty quantification, we require Monte Carlo samples of the NN-DP, which are independently drawn from its pseudo-posterior. This involves sampling the Dirichlet weights, the neighborhood specific unknown mean and covariance matrix parameters of the Gaussian kernel, and evaluating a Gaussian density for each neighborhood, as outlined in Algorithm 1. To obtain M Monte Carlo samples, the combined complexity of this step is thus $\mathcal{O}(Mn + Mnp^3) = \mathcal{O}(Mnp^3)$. Overall the runtime complexity to obtain NN-DP samples is therefore $\mathcal{O}(Mnp^3 + nkp^2 + np^3)$. For high dimensional scenarios, this runtime can be greatly improved by using a low rank matrix factorization of both the neighborhood specific empirical covariance matrix and the sampled covariance matrix parameter to make matrix inversion more efficient (Golub and van Loan, 1996). Next, we provide a detailed simulation study of runtimes of the proposed method.

In our experiments, we focus on $p = 1$ and $p = 4$. The runtime for NN-DP consists of the

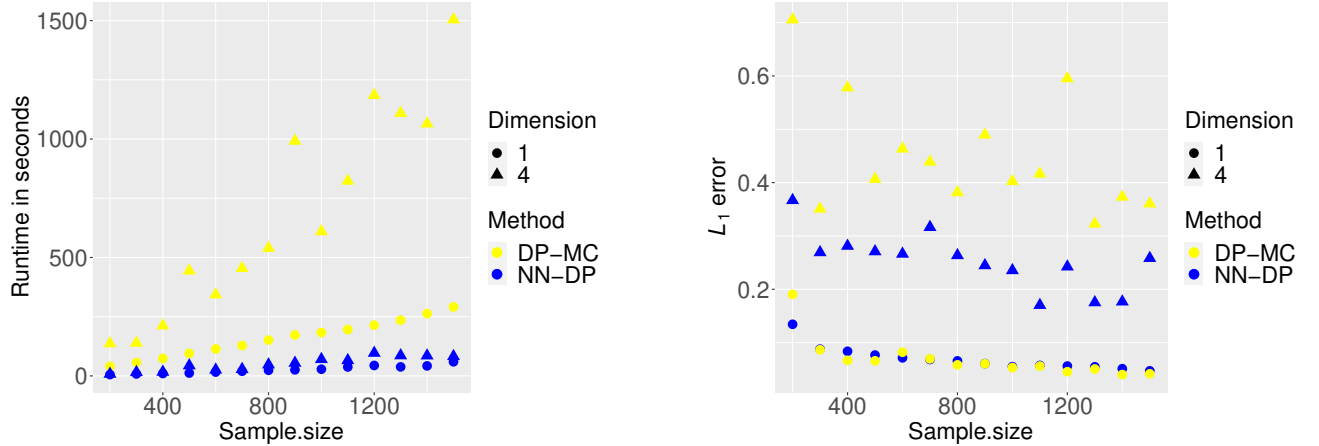


Figure 5: Runtime comparison of MCMC implementation of DPM and NN-DP in univariate case and for 4-dimensional data. Left panel shows runtimes whereas right panel shows corresponding \mathcal{L}_1 error. Sample size n is varied from 200 to 1500 in increments of 100.

time to estimate δ_0^2 by cross validation and then drawing samples from the pseudo-posterior. For both dimensions, the sample size is varied from $n = 200$ to $n = 1500$ in increments of 100. Data are generated from the standard Gaussian density (GS) for $p = 1$ and from a mixture of skew t-distributions with the parameters as described for the case MST in Section 4.3 for $p = 4$. For $p = 1$, we evaluated the two methods at 500 test points, while for $p = 4$ we evaluated the methods at 200 test points. The hyperparameters were kept the same as in Sections 4.2 and 4.3. The simulations were carried out on an i7-8700K processor with 16 gigabytes of memory.

In the left panel of Figure 5, we plot the average run time of each approach for 10 independent replications. The corresponding average \mathcal{L}_1 error of the two methods is also included in the right panel of Figure 5. The NN-DP is at least an order of magnitude faster than DP-MC. The time saved becomes more pronounced in the multivariate case, where for sample size 1500 the NN-DP is ~ 15 times faster. The gain in computing time does not come at the cost of accuracy as can be seen from the right panel; the proposed method maintains the same order of \mathcal{L}_1 error as the DP-MC in the univariate case and often outperforms the DP-MC in the multivariate case. We did not implement the Monte Carlo sampler for the proposed algorithm in parallel, but such a modification would substantially improve runtime. Bypassing cross-validation and choosing default hyperparameters instead as outlined in Section 4.1, NN-DP took 7.7 seconds and 28.4 seconds when $p = 1$ and $p = 4$, respectively, with sample size $n = 1500$. In the same scenario, DP-MC took 291.3 seconds and 1504.4 seconds for $p = 1$ and $p = 4$, respectively. Thus the NN-DP is about 38 times faster when $p = 1$ and about 53 times faster when $p = 4$.

5 Application

We apply the proposed density estimator to binary classification. Consider data $\mathcal{D} = \{(X_i, Y_i) : i = 1, \dots, n\}$, where $X_i \in \mathbb{R}^p$ are p -dimensional feature vectors and $Y_i \in \{0, 1\}$ are binary class labels. To predict the probability that $y_0 = 1$ for a test point x_0 , we use Bayes rule:

$$\text{pr}(y_0 = 1 \mid x_0) = \frac{\tilde{f}_1(x_0) \text{pr}(y_0 = 1)}{\tilde{f}_0(x_0) \text{pr}(y_0 = 0) + \tilde{f}_1(x_0) \text{pr}(y_0 = 1)}, \quad (12)$$

where $\tilde{f}_j(x_0)$ is the feature density at x_0 in class j and $\text{pr}(y_0 = j)$ is the marginal probability of class j , for $j = 0, 1$. Based on n_t test data, we let $\hat{\text{pr}}(y_0 = 1) = (1/n_t) \sum_{i=1}^{n_t} Y_i$, with $\hat{\text{pr}}(y_0 = 0) = 1 - \hat{\text{pr}}(y_0 = 1)$, and use either the nearest neighbor-Dirichlet process pseudo-posterior mean $\hat{f}_n(\cdot)$, the posterior mean of the MCMC implementation of the Dirichlet process mixture $\hat{f}_{\text{DP}}(\cdot)$ or the posterior mean of the variational Bayes approximation to the DPM $\hat{f}_{\text{VB}}(\cdot)$ for estimating the within class densities. We omit the kernel density estimator as to the best of our knowledge, no routine R implementation is available for data having more than 6 dimensions. We compare the resulting classification performances in terms of sensitivity, specificity and probabilistic calibration.

The high time resolution universe survey data (Keith et al., 2010) contain information on sampled pulsar stars. Pulsar stars are a type of neutron star and their radio emissions are detectable from the Earth. These stars have gained considerable interest from the scientific community due to their several applications (Lorimer and Kramer, 2012). The data are publicly available from the University of California at Irvine machine learning repository. Stars are classified into pulsar and non-pulsar groups according to 8 attributes (Lyon, 2016). There are a total of 17898 instances of stars, among which 1639 are classified as pulsar stars.

We create a test data set of 200 stars, among which 23 are pulsar stars. The training size is then varied from 300 to 1800 in increments of 300, each time adding 300 training points by randomly sampling from the entire data leaving out the initial test set. In Figure 6, we plot the sensitivity and specificity of the three methods in consideration. All the methods exhibit similar sensitivity across various training sizes; the Dirichlet process mixture has marginally better specificity for training sizes 1200 and 1500, while the nearest neighbor-Dirichlet process has better specificity for training sizes 300 and 600. Both NN-DP and the MCMC implementation of the DPM exhibit higher specificity and sensitivity than the variational implementation of the DPM across all training sample sizes considered.

We also compare the methods using the Brier score, a proper scoring rule (Gneiting and Raftery, 2007) for probabilistic classification. Suppose for n_t test points and the i th Monte Carlo sample, p_i denotes the sampled $n_t \times 1$ probability vector for a generic method. We compute the normalized Brier score for the i th sample as $(1/n_t) \|p_i - Y_t\|_2^2$, where Y_t is the vector of

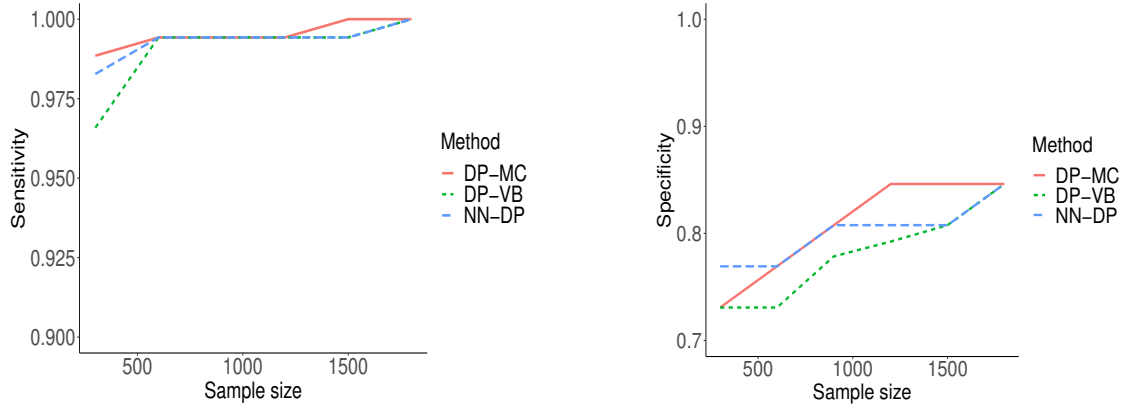


Figure 6: Sensitivity and specificity of the nearest neighbor-Dirichlet process and the Dirichlet process mixture classifiers for the universe survey data.

class labels in the test set. Then with T samples of p_i , $i = 1, \dots, T$, we compute the mean Brier score for the three methods considered. The mean Brier score for each training size is shown in the right panel of Figure 7, which naturally shows a declining trend with increasing training size. There is little to choose between the three classifiers in terms of mean Brier score; the proposed method fairs equally well in terms of calibration of estimated test set probabilities with the MCMC implementation of the Dirichlet process. In the left panel of Figure 7, the receiver operating characteristic curve of the methods is shown for 1800 training samples. The area under the curve (AUC) for the nearest neighbor-Dirichlet process, the MCMC implementation of the DPM and the variational Bayes approximation to the DPM are 0.96, 0.95 and 0.96, respectively. For 1800 training samples, the computation time for the proposed method is about 13 minutes while for the MCMC implementation of the Dirichlet process mixture it is approximately 5 hours.

Hence, the proposed method is much faster, even without exploiting parallel computation. We also fitted the proposed method using the training set of all 17698 points; MCMC implementation of the Dirichlet process mixture was too slow in this case. The sensitivity and specificity of the proposed method increased to 0.99 and 0.91, respectively.

6 Discussion

The proposed nearest neighbor-Dirichlet process provides a practically useful alternative to Dirichlet process mixtures with much faster computational speed and stability in avoiding Markov chain Monte Carlo algorithms. Such algorithms can have very poor performance in mixture models and other multimodal cases, due to difficulty in mixing, and hence can lead to posterior inferences that are unreliable. There is a recent literature attempting to scale up MCMC-based analyses in model-based clustering contexts including for Dirichlet

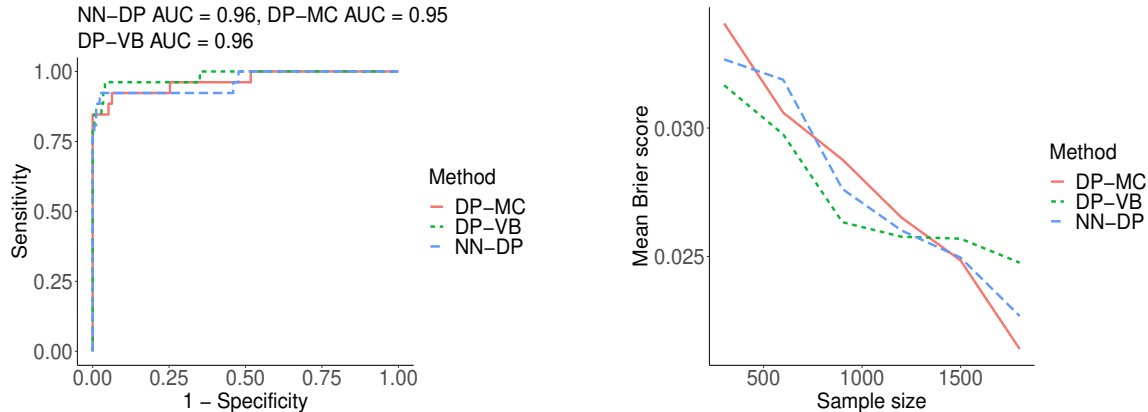


Figure 7: Left plot shows the receiver operating characteristic curve of the nearest neighbor-Dirichlet process and the Dirichlet process mixture classifiers with 1800 training samples. Area under the curve is abbreviated as AUC. Right plot shows normalized Brier scores for the methods with varying training sample size.

process mixtures; refer, for example to [Song et al. \(2020\)](#) and [Ni et al. \(2020\)](#). However, these approaches are complex to implement and are primarily focused on the problem of clustering, while we are instead focused on flexible modeling of unknown densities.

The main conceptual disadvantage of the proposed approach is the lack of a coherent Bayesian posterior updating rule. However, we have shown that nonetheless the resulting pseudo-posterior can have appealing behavior in terms of frequentist asymptotic properties, finite sample performance, and accuracy in uncertainty quantification. In addition, it is important to keep in mind that Dirichlet process mixtures and other related Bayesian non-parametric models have key disadvantages that are difficult to remove within a fully coherent Bayesian modeling framework. These include a strong sensitivity to the choice of kernel and prior on the weights on these kernels; refer, for example to [Miller and Dunson \(2019\)](#).

There are several important next steps. The first is to develop fast and robust algorithms for using the nearest neighbor-Dirichlet process not just for density estimation but also as a component of more complex hierarchical models. For example, one may want to model the residual density in regression nonparametrically or treat a random effects distribution as unknown. In such settings, one can potentially update other parameters within a Bayesian model using Markov chain Monte Carlo, while using algorithms related to those proposed in this article to update the nonparametric part conditionally on these other parameters.

7 Acknowledgements

Code used in experiments is available at <https://github.com/shounakchattopadhyay/NN-DP>. This research was partially supported by grants R01ES027498 and R01ES028804 of the

United States National Institutes of Health and grant N00014-16-1-2147 of the Office of Naval Research.

References

- Azzalini, A. (2005). The skew-normal distribution and related multivariate families. *Scandinavian Journal of Statistics*, 32(2):159–188.
- Biau, G. and Devroye, L. (2015). *Lectures on the Nearest Neighbor Method*. Springer.
- Blei, D. M. and Jordan, M. I. (2006). Variational inference for Dirichlet process mixtures. *Bayesian Analysis*, 1(1):121–143.
- Bowman, A. W. (1984). An alternative method of cross-validation for the smoothing of density estimates. *Biometrika*, 71(2):353–360.
- Devroye, L. and Györfi, L. (1985). *Nonparametric Density Estimation: the L_1 view*. Wiley Series in Probability and Statistics.
- Duong, T. (2020). *ks: Kernel Smoothing*. R package version 1.11.7.
- Escobar, M. D. and West, M. (1995). Bayesian density estimation and inference using mixtures. *Journal of the American Statistical Association*, 90(430):577–588.
- Evans, D., Jones, A. J., and Schmidt, W. M. (2002). Asymptotic moments of near-neighbour distance distributions. *Proceedings of the Royal Society of London. Series A: Mathematical, Physical and Engineering Sciences*, 458(2028):2839–2849.
- Ferguson, T. S. (1973). A Bayesian analysis of some nonparametric problems. *The Annals of Statistics*, 1(2):209–230.
- Ghosal, S., Ghosh, J. K., Ramamoorthi, R., et al. (1999). Posterior consistency of Dirichlet mixtures in density estimation. *The Annals of Statistics*, 27(1):143–158.
- Ghosal, S., Van Der Vaart, A., et al. (2007). Posterior convergence rates of Dirichlet mixtures at smooth densities. *The Annals of Statistics*, 35(2):697–723.
- Ghosal, S., Van Der Vaart, A. W., et al. (2001). Entropies and rates of convergence for maximum likelihood and Bayes estimation for mixtures of normal densities. *The Annals of Statistics*, 29(5):1233–1263.
- Gneiting, T. and Raftery, A. E. (2007). Strictly proper scoring rules, prediction, and estimation. *Journal of the American Statistical Association*, 102(477):359–378.

- Golub, G. H. and van Loan, C. F. (1996). *Matrix Computations*. John Hopkins University Press, 3 edition.
- Hahn, P. R., Martin, R., and Walker, S. G. (2018). On recursive bayesian predictive distributions. *Journal of the American Statistical Association*, 113(523):1085–1093.
- Hall, P. (1987). On Kullback-Leibler loss and density estimation. *The Annals of Statistics*, 15(4):1491–1519.
- Ishwaran, H. and James, L. F. (2001). Gibbs sampling methods for stick-breaking priors. *Journal of the American Statistical Association*, 96(453):161–173.
- Ishwaran, H. and Zarepour, M. (2002). Dirichlet prior sieves in finite normal mixtures. *Statistica Sinica*, 12(3):941–963.
- J. Ross, G. and Markwick, D. (2019). *dirichletprocess: Build Dirichlet Process Objects for Bayesian Modelling*. R package version 0.3.1.
- Jain, S. and Neal, R. M. (2004). A split-merge Markov chain Monte Carlo procedure for the Dirichlet process mixture model. *Journal of Computational and Graphical Statistics*, 13(1):158–182.
- Jara, A., Hanson, T., Quintana, F., Müller, P., and Rosner, G. (2011). DPpackage: Bayesian semi- and nonparametric modeling in R. *Journal of Statistical Software*, 40(5):1–30.
- Keith, M., Jameson, A., Van Straten, W., Bailes, M., Johnston, S., Kramer, M., Possenti, A., Bates, S., Bhat, N., Burgay, M., et al. (2010). The High Time Resolution Universe Pulsar Survey I, System configuration and initial discoveries. *Monthly Notices of the Royal Astronomical Society*, 409(2):619–627.
- Lavine, M. (1992). Some aspects of Polya tree distributions for statistical modelling. *Annals of Statistics*, 20(3):1222–1235.
- Lavine, M. (1994). More aspects of Polya tree distributions for statistical modelling. *The Annals of Statistics*, 22(3):1161–1176.
- Lo, A. Y. (1984). On a class of Bayesian nonparametric estimates: I. density estimates. *The Annals of Statistics*, 12(1):351–357.
- Loftsgaarden, D. O. and Quesenberry, C. P. (1965). A nonparametric estimate of a multivariate density function. *The Annals of Mathematical Statistics*, 36(3):1049–1051.
- Lorimer, D. R. and Kramer, M. (2012). *Handbook of Pulsar Astronomy*.

- Lyon, R. J. (2016). *Why are pulsars hard to find?* PhD thesis, The University of Manchester (United Kingdom).
- Ma, H. and Li, J. (2019). A true $O(n \log n)$ algorithm for the all-k-nearest-neighbors problem. In *International Conference on Combinatorial Optimization and Applications*, pages 362–374. Springer.
- Mack, Y. and Rosenblatt, M. (1979). Multivariate k-nearest neighbor density estimates. *Journal of Multivariate Analysis*, 9(1):1–15.
- Mildenberger, T. and Weinert, H. (2012). The benchden package: Benchmark densities for nonparametric density estimation. *Journal of Statistical Software*, 46(14):1–14.
- Miller, J. W. and Dunson, D. B. (2019). Robust Bayesian inference via coarsening. *Journal of the American Statistical Association*, 114(527):1113–1125.
- Neal, R. M. (2000). Markov chain sampling methods for Dirichlet process mixture models. *Journal of Computational and Graphical Statistics*, 9(2):249–265.
- Newton, M. A. (2002). On a nonparametric recursive estimator of the mixing distribution. *Sankhyā: The Indian Journal of Statistics, Series A*, 64(2):306–322.
- Newton, M. A. and Zhang, Y. (1999). A recursive algorithm for nonparametric analysis with missing data. *Biometrika*, 86(1):15–26.
- Ni, Y., Ji, Y., and Müller, P. (2020). Consensus monte carlo for random subsets using shared anchors. *Journal of Computational and Graphical Statistics*, 29(4):1–12.
- Papaspiliopoulos, O. and Roberts, G. O. (2008). Retrospective Markov chain Monte carlo methods for Dirichlet process hierarchical models. *Biometrika*, 95(1):169–186.
- Pólya, G. (1920). Über den zentralen grenzwertsatz der wahrscheinlichkeitsrechnung und das momentenproblem. *Mathematische Zeitschrift*, 8(3-4):171–181.
- R Core Team (2018). *R: A Language and Environment for Statistical Computing*. R Foundation for Statistical Computing, Vienna, Austria.
- Rivoirard, V. and Rousseau, J. (2012). Bernstein–von Mises theorem for linear functionals of the density. *The Annals of Statistics*, 40(3):1489–1523.
- Sethuraman, J. (1994). A constructive definition of Dirichlet priors. *Statistica Sinica*, 4(2):639–650.

- Sheather, S. J. and Jones, M. C. (1991). A reliable data-based bandwidth selection method for kernel density estimation. *Journal of the Royal Statistical Society: Series B (Methodological)*, 53(3):683–690.
- Shen, W., Tokdar, S. T., and Ghosal, S. (2013). Adaptive Bayesian multivariate density estimation with Dirichlet mixtures. *Biometrika*, 100(3):623–640.
- Song, H., Wang, Y., and Dunson, D. B. (2020). Distributed Bayesian clustering using finite mixture of mixtures. *arXiv preprint*, page arXiv:2003.13936.
- Song, P. X.-K. (2000). Multivariate dispersion models generated from Gaussian copula. *Scandinavian Journal of Statistics*, 27(2):305–320.
- Teschl, G. (2009). Mathematical methods in quantum mechanics. *Graduate Studies in Mathematics*, 99:106.
- Vaidya, P. M. (1986). An optimal algorithm for the all-nearest-neighbors problem. In *27th Annual Symposium on Foundations of Computer Science*, pages 117–122.
- Walker, S. G., Lijoi, A., and Prünster, I. (2007). On rates of convergence for posterior distributions in infinite-dimensional models. *The Annals of Statistics*, 35(2):738–746.
- Wand, M. P. and Jones, M. C. (1994). Multivariate plug-in bandwidth selection. *Computational Statistics*, 9(2):97–116.
- Wang, L. and Dunson, D. B. (2011). Fast Bayesian inference in Dirichlet process mixture models. *Journal of Computational and Graphical Statistics*, 20(1):196–216.
- Wong, W. H. and Ma, L. (2010). Optional Polya tree and Bayesian inference. *The Annals of Statistics*, 38(3):1433–1459.
- Zhang, X., Nott, D. J., Yau, C., and Jasra, A. (2014). A sequential algorithm for fast fitting of Dirichlet process mixture models. *Journal of Computational and Graphical Statistics*, 23(4):1143–1162.

Appendix

A Prerequisites

We first introduce some notation with accompanying technical details which will be used hereafter. We define the Frobenius norm of the $p \times p$ matrix A with real-valued entries by $\|A\|_F = \{\text{tr}(A^T A)\}^{1/2}$. We observe that, for a vector $v \in \mathbb{R}^p$, one has $\|vv^T\|_F = \|v\|_2^2$ where $\|a\|_2 = (a^T a)^{1/2}$ is the Euclidean norm of a . For two symmetric $p \times p$ matrices A and B , we say that $A \geq B$ if $A - B$ is positive semi-definite, that is $x^T(A - B)x \geq 0$ for all $x \in \mathbb{R}^p, x \neq 0_p$ where $0_p = (0, \dots, 0)^T$. For a symmetric matrix A_* , let the eigenvalues of A_* be denoted by $e_1(A_*), \dots, e_p(A_*)$, arranged such that $e_1(A_*) \geq \dots \geq e_p(A_*)$. If $A \geq B$, then it follows by the min-max theorem (Teschl, 2009) that, for each $j = 1, \dots, p$, we have $e_j(A) \geq e_j(B)$. In particular, we have $|A| \geq |B|$ and $\|A\|_F \geq \|B\|_F$.

Now consider independent and identically distributed data $X_1, \dots, X_n \sim f_0$ supported on the interval $[0, 1]^p$ and satisfying Assumptions 3.1-3.3 as mentioned in Section 3.1. Let $\mathcal{X}^{(n)} = (X_1, \dots, X_n)$ and suppose f_0 induces the measure P_{f_0} on the Borel σ -field on \mathbb{R}^p , denoted by $\mathcal{B}(\mathbb{R}^p)$. We form the k -nearest neighborhood of X_i using the Euclidean norm for $i = 1, \dots, n$. For a generic X_i , let Q_i be its k -th nearest neighbor in $\mathcal{X}^{-i} = (X_1, \dots, X_{i-1}, X_{i+1}, \dots, X_n)$ and let R_i be the distance between X_i and Q_i , given by $R_i = \|X_i - Q_i\|_2$. Define the ball $B_i = \{y \in [0, 1]^p : 0 < \|y - X_i\|_2 < R_i\}$ and the probability $G(X_i, R_i) = \int_{B_i} f_0(u) du$ of the ball B_i . Let $Y_1^{(i)} = X_i$ and $Y_2^{(i)}, \dots, Y_{k-1}^{(i)}$ denote the sample points which fall in B_i . Then, we define the neighborhood specific empirical mean and covariance matrix as $\bar{X}_i = k^{-1} \{\sum_{j=1}^{k-1} Y_j^{(i)} + Q_i\}$ and $S_i = k^{-1} \{\sum_{j=1}^{k-1} (Y_j^{(i)} - \bar{X}_i)(Y_j^{(i)} - \bar{X}_i)^T + (Q_i - \bar{X}_i)(Q_i - \bar{X}_i)^T\}$, respectively. Note that the random vector $(Y_2^{(i)}, \dots, Y_{k-1}^{(i)}, Q_i)$ is identically distributed for $i = 1, \dots, n$ since X_1, \dots, X_n are independent and identically distributed. Thus we only consider the case $i = 1$ from here on. For sake of brevity, denote by $Y_u = Y_u^{(1)}$ for $u = 2, \dots, k-1$ and by $Q = Q_1$.

Conditional on $X_1 = x_1 \in [0, 1]^p$ and $R_1 = r_1 > 0$, following Mack and Rosenblatt (1979) the conditional joint density of Y_2, \dots, Y_{k-1} and Q is

$$p(y_2, \dots, y_{k-1}, q \mid x_1, r_1) = \left\{ \prod_{j=2}^{k-1} \frac{f_0(y_j)}{G(x_1, r_1)} \mathbb{1}_{\{y_j \in B_1\}} \right\} \frac{f_0(q)}{G'(x_1, r_1)} \mathbb{1}_{\{\|q - x_1\| = r_1\}}, \quad (13)$$

where $G'(x_1, r_1) = \partial G(x_1, r_1) / \partial r_1$ and $\mathbb{1}_A$ denotes the indicator function of the event $A \in \mathcal{B}(\mathbb{R}^p)$. Thus conditional on X_1 and R_1 , the random variables Y_2, \dots, Y_{k-1} are independent and identically distributed, and independent of Q . Also, Mack and Rosenblatt (1979) states that under Assumptions 3.1-3.3 which imply f_0 is bounded and continuous on $[0, 1]^p$, we have

$$G(x_1, r_1) = C_p f_0(x_1) r_1^p + o(r_1^p), \quad (14)$$

as $n \rightarrow \infty$ and $r_1 \rightarrow 0$, where $C_p = [\Gamma\{(p+2)/2\}]^{-1}\pi^{p/2}$ is the volume of the unit ball in \mathbb{R}^p . Let the function $\rho(x_1, r_1) = r_1^{\kappa_1}$ where κ_1 is a non-negative integer. This function can be identified with $\phi(\cdot)$ in equation (11) of [Mack and Rosenblatt \(1979\)](#). In the following propositions we will require the expected values of $\rho(x_1, r_1)$ for different choices of κ_1 . To that end, we shall repeatedly make use of the equation (12) from [Mack and Rosenblatt \(1979\)](#) adapted to our setting:

$$E_{P_{f_0}}\{\rho(x_1, R_1) \mid X_1 = x_1\} = \frac{(n-1)!}{(k-2)!(n-k)!} \int_0^1 \left\{ \left(\frac{t}{C_p f_0(x_1)} \right)^{\kappa_1/p} + o(t^{\kappa_1/p}) \right\} t^{k-2} (1-t)^{n-k} dt. \quad (15)$$

B Proof of Theorem 3.4

Suppose X_1, \dots, X_n are independent and identically distributed random variables generated from the density f_0 supported on $[0, 1]^p$ satisfying Assumptions 3.1-3.3. For $i = 1, \dots, n$, recall the definitions of $\mu_i = \mu_i$ and $\Lambda_i = \Lambda_i$ from equation (8):

$$\mu_i = \frac{\nu_0}{\nu_n} \mu_0 + \frac{k}{\nu_n} \bar{X}_i, \quad \Lambda_i = \frac{\nu_n + 1}{\nu_n(\gamma_n - p + 1)} \Psi_i.$$

We want to show that $\hat{f}_n(x) = (1/n) \sum_{i=1}^n t_{\gamma_n-p+1}(x; \mu_i, \Lambda_i) \rightarrow f_0(x)$ in P_{f_0} -probability as $n \rightarrow \infty$ for any $x \in [0, 1]^p$, where $\hat{f}_n(x)$ is as described in (8). We first prove two propositions involving successive mean value theorem type approximations to $\hat{f}_n(x)$, which will imply the final result. We now state the two propositions, with accompanying proofs, before stating the final theorem.

Proposition B.1. *Fix $x \in [0, 1]^p$. Let $f_A(x) = (1/n) \sum_{i=1}^n t_{\gamma_n-p+1}(x; X_i, \Lambda_i)$. Also, let $k = o(n^{i_1})$ with $i_1 = 2/(p^2 + p + 2)$ and $\nu_0 = o(n^{-1/p} k^{(1/p)+1})$. Then, we have $E_{P_{f_0}}(|\hat{f}_n(x) - f_A(x)|) \rightarrow 0$ as $n \rightarrow \infty$.*

Proof. Since the $(\Lambda_i)_{i=1}^n$ are identically distributed and $(\mu_i)_{i=1}^n$ are identically distributed, we have $E_{P_{f_0}}(|\hat{f}_n(x) - f_A(x)|) \leq E_{P_{f_0}}\{|t_{\gamma_n-p+1}(x; \mu_1, \Lambda_1) - t_{\gamma_n-p+1}(x; X_1, \Lambda_1)|\}$. The multivariate mean value theorem now implies that

$$E_{P_{f_0}}(|\hat{f}_n(x) - f_A(x)|) \leq E_{P_{f_0}} \left\{ |\Lambda_1|^{-1/2} \|\nabla t_{\gamma_n-p+1}(\xi; 0_p, I_p)\|_2 \|\Lambda_1^{-1/2}(X_1 - \mu_1)\|_2 \right\}, \quad (16)$$

where $\nabla t_{\gamma_n-p+1}(\xi; 0_p, I_p) = [\partial t_{\gamma_n-p+1}(x; 0_p, I_p)/\partial x]_\xi$ for some ξ in the convex hull of $\Lambda_1^{-1/2}(x - X_1)$ and $\Lambda_1^{-1/2}(x - \mu_1)$.

Using standard results and the min-max theorem, we have

$$\|\Lambda_1^{-1/2}(X_1 - \mu_1)\|_2 \leq \|\Lambda_1^{-1/2}\|_F \|X_1 - \mu_1\|_2.$$

If we let $H_n = H = \{\nu_n(\gamma_n - p + 1)\}^{-1}(\nu_n + 1)\Psi_0 = h^2 I_p$ where $h^2 = h_n^2 = \{\nu_n(\gamma_n - p + 1)\}^{-1}\{(\nu_n + 1)(\gamma_0 - p + 1)\} \delta_0^2$ following the choice of Ψ_0 from Section 2.3, then it is clear that $\Lambda_1 \geq H$. Therefore, we have $\|\Lambda_1^{-1/2}(X_1 - \mu_1)\|_2 \leq \|H^{-1/2}\|_F \|X_1 - \mu_1\|_2$. Straightforward calculations show that $\|H^{-1/2}\|_F = h^{-1}p^{1/2}$ and $\|X_1 - \mu_1\|_2 \leq R_1 + \{\nu_n^{-1}(1 + \|\mu_0\|_2)\nu_0\}$ where $R_1 = \|X_1 - X_{1[k]}\|_2$. Using Theorem 2.4 from Biau and Devroye (2015) for $p \geq 2$ and (15) for $p = 1$, one gets

$$E_{P_{f_0}}(R_1^2) \leq d_p^2 \left(\frac{k}{n}\right)^{2/p}, \quad (17)$$

for an appropriate constant $d_p > 0$. Thus, we have $E_{P_{f_0}}(R_1) \leq \{E_{P_{f_0}}(R_1^2)\}^{1/2} \leq d_p(k/n)^{1/p}$ for sufficiently large n . This implies that

$$E(\|X_1 - \mu_1\|_2) \leq d_p \left(\frac{k}{n}\right)^{1/p} + o\left(\left(\frac{k}{n}\right)^{1/p}\right). \quad (18)$$

We also have $|\Lambda_1|^{-1/2} \leq |H|^{-1/2} = h^{-p}$. Finally, simple calculations yield that

$$\|\nabla t_{\gamma_n-p+1}(\xi; 0_p, I_p)\|_2 \leq L_{1,n,p}$$

where $L_{1,n,p} > 0$ satisfies $L_{1,n,p} \rightarrow (2\pi)^{-p/2}e^{-1/2}$ as $n \rightarrow \infty$.

Plugging all these back in (16), we obtain a finite constant $L_{2,n,p} > 0$ such that

$$E_{P_{f_0}}(|\hat{f}_n(x) - f_A(x)|) \leq L_{2,n,p}(n^{-i_1}k)^{(p^2+p+2)/(2p)} + o\{(n^{-i_1}k)^{(p^2+p+2)/(2p)}\}, \quad (19)$$

which goes to 0 as $n \rightarrow \infty$, completing the proof. \square

We now provide the second mean value theorem type approximation which approximates the random bandwidth matrix Λ_i in $f_A(x)$ by $H = H_n$ for each $i = 1, \dots, n$.

Proposition B.2. Fix $x \in [0, 1]^p$. Let $f_K(x) = (1/n) \sum_{i=1}^n t_{\gamma_n-p+1}(x; X_i, H)$. Also, let $k = o(n^{i_2})$ with $i_2 = 4/(p+2)^2$ and $\nu_0 = o\{n^{-2/p}k^{(2/p)+1}\}$. Then, we have $E_{P_{f_0}}(|f_A(x) - f_K(x)|) \rightarrow 0$ as $n \rightarrow \infty$.

Proof. Using the identically distributed properties of $(\Lambda_i)_{i=1}^n$ and $(X_i)_{i=1}^n$, we obtain $E_{P_{f_0}}(|f_A(x) - f_K(x)|) \leq E_{P_{f_0}}(|t_{\gamma_n-p+1}(x; X_1, \Lambda_1) - t_{\gamma_n-p+1}(x; X_1, H)|)$. Using the multivariate mean value

theorem, we obtain that

$$E_{P_{f_0}}(|t_{\gamma_n-p+1}(x; X_1, \Lambda_1) - t_{\gamma_n-p+1}(x; X_1, H)|) \leq E_{P_{f_0}}(\|M_1\|_F \|\Lambda_1 - H\|_F), \quad (20)$$

where $M_1 = [\partial\{t_{\gamma_n-p+1}(x; X_1, \Sigma)\}/\partial\Sigma]_{\Sigma_0}$ for some Σ_0 , with Σ_0 in the convex hull of Λ_1 and H . Since $\Lambda_1 \geq H$, we immediately have $\Sigma_0 \geq H$ as well. Using the definitions of Λ_1 and H , we have

$$\|\Lambda_1 - H\|_F \leq \frac{(\nu_n + 1)}{\nu_n(\gamma_n - p + 1)} \left\{ \left\| \sum_{j \in \mathcal{N}_1} (X_j - \bar{X}_1)(X_j - \bar{X}_1)^T \right\|_F + \frac{k\nu_0}{\nu_n} \|\bar{X}_1 \bar{X}_1^T\|_F \right\}.$$

Since $\|\sum_{j \in \mathcal{N}_1} (X_j - \bar{X}_1)(X_j - \bar{X}_1)^T\|_F \leq \sum_{j \in \mathcal{N}_1} \|(X_j - \bar{X}_1)(X_j - \bar{X}_1)^T\|_F = \sum_{j \in \mathcal{N}_1} \|X_j - \bar{X}_1\|_2^2 \leq \sum_{j \in \mathcal{N}_1} R_1^2 = kR_1^2$, we get for sufficiently large n the following:

$$E_{P_{f_0}}(\|\Lambda_1 - H\|_F) \leq E_{P_{f_0}}(R_1^2) + o\left(\frac{k}{n}\right)^{2/p}, \quad (21)$$

$$\leq d_p^2 \left(\frac{k}{n}\right)^{2/p} + o\left(\frac{k}{n}\right)^{2/p}, \quad (22)$$

using (17) and $\nu_0 = o\{n^{-2/p}k^{(2/p)+1}\}$. Taking partial derivatives of $\log\{t_{\gamma_n-p+1}(x; X_1, \Sigma)\}$ with respect to Σ evaluated at Σ_0 and taking Frobenius norm of both sides, we obtain

$$\|t_{\gamma_n-p+1}^{-1}(x; X_1, \Sigma_0) M_1\|_F \leq h^{-2}(\gamma_n + 1)$$

for sufficiently large n . We now observe that

$$t_{\gamma_n-p+1}(x; X_1, \Sigma_0) \leq c_{p, \gamma_n-p+1} |\Sigma_0|^{-1/2} \leq c_{p, \gamma_n-p+1} |H|^{-1/2} = h^{-p} c_{p, \gamma_n-p+1},$$

where $c_{p, \beta} = (\pi\beta)^{-p/2} \{\Gamma(\beta/2)\}^{-1} \Gamma\{(\beta+p)/2\}$ for $p \geq 1, \beta > 0$. Note that $c_{p, \beta} \rightarrow (2\pi)^{-p/2}$ as $\beta \rightarrow \infty$ for any $p \geq 1$. This immediately implies that $\|M_1\|_F \leq h^{-(p+2)} c_{p, \gamma_n-p+1} (\gamma_n + 1)$ for sufficiently large n . Plugging all these back in equation (20), we obtain for sufficiently large n , a finite $L_{3, n, p} > 0$ such that

$$E_{P_{f_0}}(|f_A(x) - f_K(x)|) \leq L_{3, n, p} (n^{-i_2} k)^{(p+2)^2/(2p)} + o\{(n^{-i_2} k)^{(p+2)^2/(2p)}\}, \quad (23)$$

which goes to 0 as $n \rightarrow \infty$, proving the proposition. \square

We now prove Theorem 3.4.

Theorem 4. $E_{P_{f_0}}(|\hat{f}_n(x) - f_K(x)|) \leq E_{P_{f_0}}(|\hat{f}_n(x) - f_A(x)|) + E_{P_{f_0}}(|f_A(x) - f_K(x)|)$ by the triangle inequality. Using Propositions B.1 and B.2, we obtain that $E_{P_{f_0}}(|\hat{f}_n(x) - f_K(x)|) \rightarrow 0$ as $n \rightarrow \infty$. From Section E of the Appendix, we obtain $f_K(x) \rightarrow f_0(x)$ in P_{f_0} -probability. This immediately implies that given the conditions on k, ν_0 and for any $x \in [0, 1]^p$, we have $\hat{f}_n(x) \rightarrow f_0(x)$ in P_{f_0} -probability. \square

C Proof of Theorem 3.5

Proof. Fix $x \in [0, 1]^p$. For $i = 1, \dots, n$, let $z_i = \phi_p(x; \eta_i, \Sigma_i)$ and suppose $z^{(n)} = (z_1, \dots, z_n)^T$. Then, we have $f(x) = \sum_{i=1}^n \pi_i z_i = z^{(n)T} \pi^{(n)}$ where $\pi^{(n)} = (\pi_1, \dots, \pi_n)^T \sim \text{Dirichlet}(\omega, \dots, \omega)$ given $\mathcal{X}^{(n)}$, with $\omega = \alpha + 1$. We begin with the identity

$$\text{var}\{f(x) \mid \mathcal{X}^{(n)}\} = \text{var}[E\{f(x) \mid \mathcal{X}^{(n)}, z^{(n)}\} \mid \mathcal{X}^{(n)}] + E[\text{var}\{f(x) \mid \mathcal{X}^{(n)}, z^{(n)}\} \mid \mathcal{X}^{(n)}]. \quad (24)$$

For $i = 1, \dots, n$, we have

$$E(z_i^2 \mid \mathcal{X}^{(n)}) = R_n |B_i|^{-1/2} t_{\gamma_n - p + 2}(x; \mu_i, B_i), \quad (25)$$

where

$$R_n = \frac{\Gamma\{(\gamma_n - p + 2)/2\}}{\Gamma\{(\gamma_n - p + 1)/2\}} \left[\frac{\nu_n + 2}{4\pi\nu_n(\gamma_n - p + 2)} \right]^{p/2},$$

$B_i = D_n \Lambda_i$ and $D_n = \{2(\gamma_n - p + 2)(\nu_n + 1)\}^{-1}(\gamma_n - p + 1)(\nu_n + 2)$. Equation (25) is obtained by integrating over the pseudo-posterior distribution of $(\eta_i, \Sigma_i)_{i=1}^n$ given $\mathcal{X}^{(n)}$, namely $\text{NIW}(\mu_i, \Sigma_i/\nu_n, \gamma_n, \Psi_i)$. Moreover, z_1, \dots, z_n are conditionally independent given the data $\mathcal{X}^{(n)}$.

We start with the first term on the right hand side of (24). We have

$$\begin{aligned} \text{var}[E\{f(x) \mid \mathcal{X}^{(n)}, z^{(n)}\} \mid \mathcal{X}^{(n)}] &= \text{var}\left(\frac{1}{n} \sum_{i=1}^n z_i \mid \mathcal{X}^{(n)}\right) \\ &= \frac{1}{n^2} \sum_{i=1}^n \text{var}(z_i \mid \mathcal{X}^{(n)}) \\ &\leq \frac{1}{n^2} \sum_{i=1}^n E(z_i^2 \mid \mathcal{X}^{(n)}) \\ &= \frac{1}{n^2} \sum_{i=1}^n R_n |B_i|^{-1/2} t_{\gamma_n - p + 2}(x; \mu_i, B_i), \end{aligned}$$

where the first equality is obtained using $E(\pi_i \mid \mathcal{X}^{(n)}) = 1/n$ for each $i = 1, \dots, n$ and the

last equality is obtained using equation (25). For $i = 1, \dots, n$, since $|\Lambda_i| \geq |H|$, we have $|B_i| \geq D_n^p |H|$. Letting $\hat{f}_{var}(x) = (1/n) \sum_{i=1}^n t_{\gamma_n-p+2}(x; \mu_i, B_i)$ and $a_n(x) = R_n D_n^{-p/2} \hat{f}_{var}(x)$, we have,

$$\text{var}[E\{f(x) \mid \mathcal{X}^{(n)}, z^{(n)}\} \mid \mathcal{X}^{(n)}] \leq \frac{a_n(x)}{n|H|^{1/2}}. \quad (26)$$

We now analyze the second term on the right hand side of (24). Recall that $\pi^{(n)}$ is conditionally independent of $z^{(n)}$ given the data $\mathcal{X}^{(n)}$ following from the nearest neighbor-Dirichlet process framework as discussed in Section 2.1. Let Σ_π denote the pseudo-posterior covariance matrix of $\pi^{(n)}$. Given $\mathcal{X}^{(n)}$, since $\pi^{(n)} \sim \text{Dirichlet}(\omega, \dots, \omega)$ where $\omega = \alpha + 1$, standard results yield that $\Sigma_\pi = V_n\{(1 - C_n)I_n + C_n J_n\}$, where $V_n = (n - 1)/\{n^2(n\omega + 1)\}$, $C_n = -1/(n - 1)$, I_n is the $n \times n$ identity matrix, and $J_n = 1_n 1_n^T$ where $1_n = (1, \dots, 1)^T \in \mathbb{R}^n$. Then, we have

$$E[\text{var}\{f(x) \mid \mathcal{X}^{(n)}, z^{(n)}\} \mid \mathcal{X}^{(n)}] = E[z^{(n)T} \Sigma_\pi z^{(n)} \mid \mathcal{X}^{(n)}]. \quad (27)$$

Using the expression for Σ_π along with equation (27), we obtain,

$$E[\text{var}\{f(x) \mid \mathcal{X}^{(n)}, z^{(n)}\} \mid \mathcal{X}^{(n)}] = \frac{1}{(n\omega + 1)} E\left\{ \frac{1}{n} \sum_{i=1}^n (z_i - \bar{z})^2 \mid \mathcal{X}^{(n)} \right\}, \quad (28)$$

where $\bar{z} = (1/n) \sum_{i=1}^n z_i$. We now have

$$\begin{aligned} E[\text{var}\{f(x) \mid \mathcal{X}^{(n)}, z^{(n)}\} \mid \mathcal{X}^{(n)}] &= \frac{1}{n(n\omega + 1)} \left\{ \sum_{i=1}^n E(z_i^2 \mid \mathcal{X}^{(n)}) - nE(\bar{z}^2 \mid \mathcal{X}^{(n)}) \right\} \\ &\leq \frac{1}{n(n\omega + 1)} \sum_{i=1}^n E(z_i^2 \mid \mathcal{X}^{(n)}) \\ &\leq \frac{1}{n(n\omega + 1)} \sum_{i=1}^n R_n |B_i|^{-1/2} t_{\gamma_n-p+2}(x; \mu_i, B_i), \end{aligned}$$

where the last inequality is obtained using equation (25). Using $|B_i| \geq D_n^p |H|$ for $i = 1, \dots, n$ as before, we have

$$E[\text{var}\{f(x) \mid \mathcal{X}^{(n)}, z^{(n)}\} \mid \mathcal{X}^{(n)}] \leq \frac{a_n(x)}{(n\omega + 1)|H|^{1/2}}. \quad (29)$$

Combining equations (26) and (29) and putting the results back in equation (24), we have the inequality. If we let $n \rightarrow \infty$ we immediately obtain that $\text{var}\{f(x) \mid \mathcal{X}^{(n)}\} \rightarrow 0$ in P_{f_0} -probability. \square

D Proof of Theorem 3.7 and Choice of α

D.1 Proof of Theorem 3.7

Proof. Let $\eta^{(n)} = (\eta_1, \dots, \eta_n)^\top$. Then, we have $\Theta = \sum_{i=1}^n \pi_i \eta_i = \eta^{(n)\top} \pi^{(n)}$ where $\pi^{(n)} = (\pi_1, \dots, \pi_n)^\top \sim \text{Dirichlet}(\omega, \dots, \omega)$ given $\mathcal{X}^{(n)}$, with $\omega = \alpha + 1$, and $\eta^{(n)} = (\eta_1, \dots, \eta_n)^\top$. We start out by observing that

$$\text{var}(\Theta \mid \mathcal{X}^{(n)}) = \text{var}[E\{\Theta \mid \eta^{(n)}, \mathcal{X}^{(n)}\} \mid \mathcal{X}^{(n)}] + E[\text{var}\{\Theta \mid \eta^{(n)}, \mathcal{X}^{(n)}\} \mid \mathcal{X}^{(n)}]. \quad (30)$$

Let n be sufficiently large so that $k > 2 - \gamma_0$, since $k \rightarrow \infty$ as $n \rightarrow \infty$. For $i = 1, \dots, n$, let $v_i = \text{var}(\eta_i \mid \mathcal{X}^{(n)}) = \gamma_n \delta_i^2 / \{\nu_n(\gamma_n - 2)\}$, and $\bar{v} = (1/n) \sum_{i=1}^n v_i$. Since $E\{\Theta \mid \eta^{(n)}, \mathcal{X}^{(n)}\} = (1/n) \sum_{i=1}^n \eta_i$ and η_1, \dots, η_n are conditionally independent given the data $\mathcal{X}^{(n)}$, we have

$$\text{var}[E\{\Theta \mid \eta^{(n)}, \mathcal{X}^{(n)}\} \mid \mathcal{X}^{(n)}] = \frac{\bar{v}}{n}. \quad (31)$$

Since the pseudo-posterior covariance matrix of $\pi^{(n)}$ is $\Sigma_\pi = V_n\{(1 - C_n)I_n + C_n J_n\}$, we obtain

$$\begin{aligned} \text{var}\{\Theta \mid \eta^{(n)}, \mathcal{X}^{(n)}\} &= \frac{1}{n(n\omega + 1)} \sum_{i=1}^n (\eta_i - \bar{\eta})^2 \\ &= \frac{1}{n(n\omega + 1)} \left(\sum_{i=1}^n \eta_i^2 - n \bar{\eta}^2 \right), \end{aligned} \quad (32)$$

where $\bar{\eta} = (1/n) \sum_{i=1}^n \eta_i$. Now, for $i = 1, \dots, n$, we have $E(\eta_i^2 \mid \mathcal{X}^{(n)}) = \mu_i^2 + v_i$, and $E(\bar{\eta}^2 \mid \mathcal{X}^{(n)}) = (\bar{v}/n) + \bar{\mu}^2$. Putting these back in equation (32) we get that

$$E[\text{var}\{\Theta \mid \eta^{(n)}, \mathcal{X}^{(n)}\} \mid \mathcal{X}^{(n)}] = \frac{1}{n(n\omega + 1)} \left\{ \sum_{i=1}^n (\mu_i - \bar{\mu})^2 + (n - 1) \bar{v} \right\}. \quad (33)$$

Combining the results of equations (31) and (33), putting them back in equation (30), and multiplying both sides by n , we get the result. \square

D.2 Choice of α

Suppose $\sigma_{f_0}^2$ is the variance of the underlying true density f_0 satisfying Assumptions 3.1-3.3. Let $S_\mu^2 = (1/n) \sum_{i=1}^n (\mu_i - \bar{\mu})^2$ and $S^2 = (1/n) \sum_{i=1}^n (X_i - \bar{X})^2$. We start out by observing

that

$$\begin{aligned} E_{P_{f_0}}(|S_\mu^2 - S^2|) &\leq \frac{1}{n} E_{P_{f_0}} \left\{ \sum_{i=1}^n |(\mu_i - X_i + \bar{X} - \bar{\mu})(\mu_i + X_i - \bar{\mu} - \bar{X})| \right\} \\ &\leq \frac{4}{n} E_{P_{f_0}} \left\{ \sum_{i=1}^n (|\mu_i - X_i| + |\bar{X} - \bar{\mu}|) \right\} \end{aligned}$$

by the triangle inequality and the fact that $|\mu_i|, |X_i| \leq 1$ for $i = 1, \dots, n$. Since $(\mu_i)_{i=1}^n$ are identically distributed and $(X_i)_{i=1}^n$ are identically distributed, we have

$$E_{P_{f_0}}(|S_\mu^2 - S^2|) \leq 4\{E_{P_{f_0}}(|\mu_1 - X_1|) + E_{P_{f_0}}(|\bar{\mu} - \bar{X}|)\}.$$

But $E_{P_{f_0}}(|\bar{\mu} - \bar{X}|) \leq (1/n) \sum_{i=1}^n E_{P_{f_0}}(|\mu_i - X_i|)$ by the triangle inequality, from which it follows that $E_{P_{f_0}}(|\bar{\mu} - \bar{X}|) \leq E_{P_{f_0}}(|\mu_1 - X_1|)$ since $(\mu_i - X_i)$ are identically distributed for $i = 1, \dots, n$. Thus, we have

$$\begin{aligned} E_{P_{f_0}}(|S_\mu^2 - S^2|) &\leq 8 E_{P_{f_0}}(|\mu_1 - X_1|) \\ &\leq 8d_1 \frac{k}{n} + o\left(\frac{k}{n}\right), \end{aligned} \tag{34}$$

using (18). Since $S^2 \rightarrow \sigma_{f_0}^2$ in P_{f_0} -probability as $n \rightarrow \infty$ by the weak law of large numbers, we get that $S_\mu^2 \rightarrow \sigma_{f_0}^2$ in P_{f_0} -probability as $n \rightarrow \infty$ as well. Equating the pseudo-posterior variance of $n^{1/2}\Theta$ from Theorem 3.7 with $\sigma_{f_0}^2$, we get after some rearranging,

$$\omega + \frac{1}{n} = \frac{S_\mu^2 + \{(n-1)\bar{v}/n\}}{\sigma_{f_0}^2 - \bar{v}}. \tag{35}$$

As $n \rightarrow \infty$, since each λ_i satisfies $\lambda_i^2 - h^2 \rightarrow 0$ in P_{f_0} -probability for $i = 1, \dots, n$ using equation (22) with $p = 1$, \bar{v} is well approximated by $(\gamma_n \nu_n)^{-1}(\gamma_0 \delta_0^2)$ in the sense that $\{\bar{v} - (\gamma_n \nu_n)^{-1}(\gamma_0 \delta_0^2)\} \rightarrow 0$ in P_{f_0} -probability as $n \rightarrow \infty$. In particular, we have $\bar{v} \rightarrow 0$ in P_{f_0} -probability. Combining these with the fact that $S_\mu^2 \rightarrow \sigma_{f_0}^2$ in P_{f_0} -probability as $n \rightarrow \infty$, we obtain,

$$\omega = \alpha + 1 \approx 1 + \frac{\bar{v}}{\sigma_{f_0}^2} - \frac{1}{n}. \tag{36}$$

Since $1/n$ can be asymptotically neglected in comparison to $\bar{v}/\sigma_{f_0}^2$ owing to the fact that $k^2/n \rightarrow 0$ as $n \rightarrow \infty$ for $p = 1$, (36) implies the choice of α as described in equation (11).

E Proof of Consistency of $f_K(x)$

Define the standard multivariate t-density with $d > 0$ degrees of freedom to be $g_d(x) = t_d(x; 0_p, I_p)$. Since $H = H_n$ as defined in Section 3.1 is diagonal, it immediately follows that $t_{\gamma_n-p+1}(x; x', H) = h^{-p} g_{\gamma_n-p+1}\{h^{-1}(x - x')\}$. The following lemma proves the consistency of any such generic kernel density estimator with t kernel depending on n , say

$$f_K(x) = \frac{1}{nw^p} \sum_{i=1}^n g_{\gamma_n-p+1} \left(\frac{x - X_i}{w} \right),$$

where the bandwidth $w = w_n$ satisfies $w_n \rightarrow 0$ and $nw_n^p \rightarrow \infty$ as $n \rightarrow \infty$, with independent and identically distributed data $X_1, \dots, X_n \sim f_0$ satisfying Assumptions 3.1-3.3.

Lemma E.1. *Suppose $w = w_n$ is a sequence satisfying $w \rightarrow 0$ and $nw^p \rightarrow \infty$ as $n \rightarrow \infty$. Let $f_K(x) = (nw^p)^{-1} \sum_{i=1}^n g_{\gamma_n-p+1}\{w^{-1}(x - X_i)\}$. Then $f_K(x) \rightarrow f_0(x)$ in P_{f_0} -probability for each $x \in [0, 1]^p$.*

Proof. It is enough to show that $E_{P_{f_0}}\{f_K(x)\} \rightarrow f_0(x)$ and $\text{var}_{P_{f_0}}\{f_K(x)\} \rightarrow 0$ as $n \rightarrow \infty$. Let us start first with $E_{P_{f_0}}\{f_K(x)\}$. We have

$$\begin{aligned} E_{P_{f_0}}\{f_K(x)\} &= E_{P_{f_0}} \left\{ \frac{1}{w^p} g_{\gamma_n-p+1} \left(\frac{x - X_1}{w} \right) \right\} \\ &= \int_{[0,1]^p} \frac{1}{w^p} g_{\gamma_n-p+1} \left(\frac{y - x}{w} \right) f_0(y) dy \\ &= \int_{[-\frac{x}{w}, \frac{1-x}{w}]^p} g_{\gamma_n-p+1}(u) f_0(x + wu) du, \\ &= \int_{[-\frac{x}{w}, \frac{1-x}{w}]^p} g_{\gamma_n-p+1}(u) \{f_0(x) + wu^T \nabla f_0(\xi)\} du \\ &= f_0(x) \int_{[-\frac{x}{w}, \frac{1-x}{w}]^p} g_{\gamma_n-p+1}(u) du + w \int_{[-\frac{x}{w}, \frac{1-x}{w}]^p} g_{\gamma_n-p+1}(u) u^T \nabla f_0(\xi) du, \\ &= f_0(x) \{1 - o_n(1)\} + w \mathcal{O}_n(1), \end{aligned}$$

using the mean value theorem and Polya's theorem (Pólya, 1920) along with Assumption 3.2 to bound $\nabla f_0(\cdot)$. As $n \rightarrow \infty$, this implies that $E_{P_{f_0}}\{f_K(x)\} \rightarrow f_0(x)$ since $w \rightarrow 0$ as $n \rightarrow \infty$.

The variance may be dealt with in a similar manner. Following the same steps as before

we get

$$\begin{aligned}
\text{var}_{P_{f_0}} \{f_K(x)\} &= \frac{1}{n} \text{var}_{P_{f_0}} \left\{ \frac{1}{w^p} g_{\gamma_n-p+1} \left(\frac{x - X_1}{w} \right) \right\} \leq \frac{1}{n} E_{P_{f_0}} \left\{ \frac{1}{w^{2p}} g_{\gamma_n-p+1}^2 \left(\frac{x - X_1}{w} \right) \right\} \\
&\leq \frac{1}{nw^{2p}} \int_{[0,1]^p} g_{\gamma_n-p+1}^2 \left(\frac{y-x}{w} \right) f_0(y) dy \\
&\leq \frac{1}{nw^p} \int_{[-\frac{x}{w}, \frac{1-x}{w}]^p} g_{\gamma_n-p+1}^2(u) \{f_0(x) + wu^\top \nabla f_0(\xi)\} du, \\
&\leq \frac{f_0(x) \mathcal{O}_n(1)}{nw^p},
\end{aligned}$$

which shows that the variance goes to 0 as $n \rightarrow \infty$, since $nw^p \rightarrow \infty$ as $n \rightarrow \infty$. \square

For the nearest neighbor-Dirichlet process, recall $f_K(x) = (1/n) \sum_{i=1}^n t_{\gamma_n-p+1}(x; X_i, H)$ from Section 3.1 of the main document, where $H = h^2 I_p$ and $h^2 = h_n^2 = \{\nu_n(\gamma_n - p + 1)\}^{-1} \{(\nu_n + 1)(\gamma_0 - p + 1)\} \delta_0^2$. Here, the bandwidth h_n satisfies $h_n \rightarrow 0$ and $nh_n^p \rightarrow \infty$ as $n \rightarrow \infty$. Lemma E.1 then shows that $f_K(x)$ converges to $f_0(x)$ in P_{f_0} -probability as $n \rightarrow \infty$.

F Cross-validation

Consider independent and identically distributed data $X_1, \dots, X_n \in \mathbb{R}^p \sim f$ with f having the nearest neighbor-Dirichlet process formulation. In the univariate setting, the prior for each of the neighborhood specific parameters is $\theta_i = (\eta_i, \sigma_i^2) \sim \text{NIG}(\mu_0, \sigma_i^2/\nu_0, \gamma_0/2, \gamma_0\delta_0^2/2)$. The equivalent prior in the general multivariate setting following Sections 2.2 and 2.3 is $(\eta_i, \Sigma_i) \sim \text{NIW}(\mu_0, \Sigma_i/\nu_0, \gamma_0, \Psi_0)$ where $\Psi_0 = (\gamma_*\delta_0^2) I_p$ with $\gamma_* = \gamma_0 - p + 1$. We use the pseudo-posterior mean in equations (8) and (9) to compute leave-one-out log likelihoods $\mathbf{L}(\delta_0^2)$ for different choices of the hyperparameter δ_0^2 , choosing $\delta_{0,\text{CV}}^2 = \arg \sup_{\delta_0^2} \mathbf{L}(\delta_0^2)$ to maximize this criteria. The details of the computation of $\mathbf{L}(\delta_0^2)$ for a fixed δ_0^2 are provided in Algorithm 2.

F.1 Fast Implementation of Cross-validation

In Algorithm 2, the nearest neighborhood specification for each \mathcal{X}^{-i} is different for $i = 1, \dots, n$. However, we bypass this computation by initially forming a neighborhood of size $(k+1)$ for each data point using the entire data and storing the respective neighborhood means and covariance matrices. Suppose for X_i , the indices of the $(k+1)$ -nearest neighbors are given by $\mathcal{N}_i = \{j \in \{1, \dots, n\} : \|X_i - X_j\|_2 \leq \|X_i - X_{i[k+1]}\|_2\}$, arranged in increasing order according to their distance from X_i with $X_{i[1]} = X_i$. Define the neighborhood mean $m_i = \{1/(k+1)\} \sum_{j \in \mathcal{N}_i} X_{i[j]}$ and the neighborhood covariance ma-

Algorithm 2: Leave-one-out cross-validation for choosing the hyperparameter δ_0^2 in nearest neighbor-Dirichlet process method.

- Consider data $\mathcal{X}^{(n)} = (X_1, \dots, X_n)$ where $X_i \in \mathbb{R}^p$, $p \geq 1$.

Fix the number of neighbors k and other hyperparameters μ_0, ν_0, γ_0 .

- For $i \in \{1, \dots, n\}$, consider the data set leaving out the i th data point, given by $\mathcal{X}^{-i} = (X_1, \dots, X_{i-1}, X_{i+1}, \dots, X_n)$. Compute the pseudo-posterior mean density estimate at X_i , namely $\hat{f}_{-i}(X_i)$, using \mathcal{X}^{-i} and equation (9) when $p = 1$, or equation (8) when $p \geq 2$. Write this as $\mathbf{L}_i(\delta_0^2) = \hat{f}_{-i}(X_i)$. Finally, compute the leave-one-out log likelihood given by

$$\mathbf{L}(\delta_0^2) = \frac{1}{n} \sum_{i=1}^n \log\{\mathbf{L}_i(\delta_0^2)\}.$$

- For $\delta_0^2 > 0$, obtain $\delta_{0,\text{CV}}^2 = \arg \sup_{\delta_0^2} \mathbf{L}(\delta_0^2)$.
-

trix $S_i = (k+1)^{-1} \{\sum_{j \in \mathcal{N}_i} (X_{i[j]} - m_i)(X_{i[j]} - m_i)^\top\}$. Then, to form a k -nearest neighborhood for the new data \mathcal{X}^{-i} , a single pass over the initial neighborhoods \mathcal{N}_i is sufficient to update the new neighborhood means and covariance matrices. Below, we describe the update for the neighborhood means $m_j^{(-i)}$ and covariance matrices $S_j^{(-i)}$ for $j = 1, \dots, n$ and $j \neq i$, considering the data \mathcal{X}^{-i} . For $j = 1, \dots, n$ and $j \neq i$, we have,

$$\begin{aligned} m_j^{(-i)} &= \begin{cases} (1/k)\{(k+1)m_j - X_{j[k+1]}\} & \text{if } X_i \notin \mathcal{N}_j, \\ (1/k)\{(k+1)m_j - X_i\} & \text{if } X_i \in \mathcal{N}_j. \end{cases} \\ S_j^{(-i)} &= \begin{cases} S_j - \{(k+1)/k\}(m_j - X_{j[k+1]})(m_j - X_{j[k+1]})^\top & \text{if } X_i \notin \mathcal{N}_j, \\ S_j - \{(k+1)/k\}(m_j - X_i)(m_j - X_i)^\top & \text{if } X_i \in \mathcal{N}_j. \end{cases} \end{aligned} \quad (37)$$

G Algorithm with Gaussian Kernels for Univariate Data

Suppose we have independent and identically distributed observations $\mathcal{X}^{(n)} = (X_1, \dots, X_n)$ from the density f , where $X_i \in \mathbb{R}$, $i = 1, \dots, n$. In the nearest neighbor-Dirichlet process framework for univariate data with the Gaussian kernel $\phi(\cdot; \eta, \sigma^2)$, neighborhood specific parameters $\theta_i = (\eta_i, \sigma_i^2) \sim \text{NIG}(\mu_0, \sigma_i^2/\nu_0, \gamma_0/2, \gamma_0\delta_0^2/2)$ *a priori* independently for $i = 1, \dots, n$. Monte Carlo samples for the estimated density at any point x can be generated following the steps of Algorithm 3.

Algorithm 3: Nearest neighbor-Dirichlet process algorithm to obtain Monte Carlo samples from the pseudo-posterior of $f(x)$ given univariate data $\mathcal{X}^{(n)}$ with Gaussian kernel and normal-inverse gamma prior.

- **Step 1:** Compute the neighborhood \mathcal{N}_i for data point X_i with $X_{i[1]} = X_i$, according to distance $d(\cdot, \cdot)$ with $(k - 1)$ nearest neighbors.
- **Step 2:** Update the parameters for neighborhood \mathcal{N}_i to $(\mu_i, \nu_n, \gamma_n, \delta_i^2)$ where $\nu_n = \nu_0 + k$, $\gamma_n = \gamma_0 + k$, $\mu_i = \nu_0 \nu_n^{-1} \mu_0 + k \nu_n^{-1} \bar{X}_i$, $\bar{X}_i = k^{-1} \sum_{j \in \mathcal{N}_i} X_j$ and $\delta_i^2 = \gamma_n^{-1} \left\{ \gamma_0 \delta_0^2 + \sum_{j \in \mathcal{N}_i} (X_j - \bar{X}_i)^2 + k \nu_0 \nu_n^{-1} (\mu_0 - \bar{X}_i)^2 \right\}$.
- **Step 3:** To compute the t th Monte Carlo sample of $f(x)$, sample Dirichlet weights $\pi^{(t)} \sim \text{Dirichlet}(\alpha + 1, \dots, \alpha + 1)$ and neighborhood-specific parameters $(\eta_i^{(t)}, \sigma_i^{(t)2}) \sim \text{NIG} \left(\mu_i, \sigma_i^{(t)2} / \nu_n, \gamma_n / 2, \gamma_n \delta_i^2 / 2 \right)$ independently for $i = 1, \dots, n$, and set

$$f^{(t)}(x) = \sum_{i=1}^n \pi_i^{(t)} \phi(x; \eta_i^{(t)}, \sigma_i^{(t)2}). \quad (38)$$

H Inverse Wishart Parametrization

The parametrization of the inverse Wishart density defined on the set of all $p \times p$ matrices with real entries used in this article is given as follows. Suppose $\gamma > p - 1$ and Ψ is a $p \times p$ positive definite matrix. If $\Sigma \sim \text{IW}_p(\gamma, \Psi)$, then Σ has the following density function:

$$g(\Sigma) = \begin{cases} \frac{|\Psi|^{\gamma/2}}{2^{\gamma p/2} \Gamma_p(\gamma/2)} |\Sigma|^{-(\gamma+p+1)/2} \text{etr} \left(-\frac{1}{2} \Psi \Sigma^{-1} \right) & \text{if } \Sigma \text{ is positive definite,} \\ 0 & \text{otherwise,} \end{cases}$$

where $\Gamma_p(\cdot)$ is the multivariate gamma function defined by

$$\Gamma_p(a) = \pi^{p(p-1)/4} \prod_{j=1}^p \Gamma \left(a + \frac{1-j}{2} \right)$$

for $a \geq (p - 1)/2$ and the function $\text{etr}(A) = \exp \{ \text{tr}(A) \}$ for a square matrix A .

I \mathcal{L}_1 Error Tables

Sample size	Estimator	CA	CW	DE	GS	IE	LN	LO	SB	SP	ST
200	NN-DP	0.22	0.32	0.19	0.12	0.39	0.20	0.13	0.17	0.33	0.31
	DP-MC	0.19	0.37	0.16	0.10	0.36	0.22	0.13	0.23	0.27	0.56
	KDE	-	0.37	0.16	0.12	-	0.18	0.11	0.18	-	0.52
	KNN	5.99	0.58	0.59	0.28	3.46	0.54	0.48	0.39	6.02	0.46
	DP-VB	0.20	0.35	0.15	0.08	0.53	0.25	0.11	0.11	0.44	0.57
	RD	-	0.35	0.13	0.12	-	0.16	0.11	0.16	-	0.53
	PTM	0.29	0.27	0.18	0.13	0.38	0.22	0.13	0.20	0.40	0.39
500	NN-DP	0.16	0.18	0.13	0.08	0.31	0.17	0.10	0.11	0.25	0.21
	DP-MC	0.12	0.35	0.12	0.08	0.27	0.19	0.09	0.13	0.22	0.53
	KDE	-	0.32	0.11	0.08	-	0.15	0.08	0.11	-	0.51
	KNN	3.62	0.47	0.48	0.27	3.39	0.40	0.30	0.31	5.64	0.35
	DP-VB	0.14	0.33	0.11	0.05	0.48	0.19	0.08	0.08	0.45	0.55
	RD	-	0.32	0.10	0.09	-	0.13	0.09	0.10	-	0.50
	PTM	0.24	0.19	0.14	0.10	0.32	0.19	0.11	0.14	0.32	0.30

Table 3: Comparison of the methods in terms of the expected \mathcal{L}_1 distance in the univariate case. Number of test points and replications considered are $n_t = 500$ and $R = 20$.

Density		MG				MST				MVC				MVG				SN				T			
Sample size	Dimension	2	3	4	6	2	3	4	6	2	3	4	6	2	3	4	6	2	3	4	6	2	3	4	6
200	NN-DP	0.29	0.41	0.47	0.68	0.28	0.38	0.45	0.60	0.33	0.48	0.52	0.62	0.33	0.50	0.61	0.74	0.24	0.33	0.42	0.58	0.27	0.34	0.40	0.53
	DP-MC	0.20	0.53	0.62	0.67	0.22	0.42	0.55	0.68	0.31	0.46	0.51	0.60	0.34	0.52	0.61	0.73	0.16	0.19	0.27	0.34	0.21	0.26	0.35	0.44
	KDE	0.28	0.52	0.79	1.29	0.27	0.55	0.72	1.21	-	-	-	-	0.43	0.77	0.90	1.09	0.22	0.50	0.78	1.26	0.26	0.53	0.74	1.21
	KNN	1.93	3.82	4.80	18.83	7.28	8.22	9.25	11.05	4.92	7.31	15.24	20.5	3.30	3.65	4.75	5.54	2.21	5.16	8.37	10.04	2.97	6.37	10.22	17.54
	DP-VB	0.29	0.38	0.41	0.50	0.24	0.36	0.44	0.59	0.48	0.85	1.28	1.69	0.45	0.58	0.71	0.86	0.17	0.23	0.31	0.52	0.19	0.29	0.34	0.46
1000	NN-DP	0.18	0.26	0.34	0.46	0.19	0.27	0.32	0.44	0.28	0.33	0.46	0.50	0.29	0.44	0.49	0.62	0.15	0.22	0.29	0.42	0.17	0.24	0.30	0.38
	DP-MC	0.09	0.40	0.57	0.59	0.12	0.20	0.31	0.55	0.26	0.39	0.48	0.54	0.21	0.38	0.51	0.64	0.06	0.09	0.10	0.15	0.10	0.15	0.19	0.28
	KDE	0.16	0.32	0.52	0.96	0.16	0.35	0.53	1.04	-	-	-	-	0.33	0.66	0.73	0.93	0.13	0.32	0.53	1.05	0.14	0.32	0.52	0.90
	KNN	0.92	2.62	4.01	15.28	5.96	6.48	7.04	9.63	4.68	6.29	13.7	17.04	2.01	2.59	3.88	4.09	1.89	4.39	6.84	8.15	2.37	5.30	9.66	13.28
	DP-VB	0.25	0.29	0.33	0.36	0.15	0.24	0.25	0.45	0.42	0.74	0.82	0.91	0.38	0.54	0.61	0.77	0.10	0.12	0.15	0.20	0.10	0.15	0.18	0.31

Table 4: Comparison of the methods in terms of the \mathcal{L}_1 distance in the multivariate case. Number of test points and replications considered are $n_t = 500$ and $R = 20$.